การจำลองพลวัตเชิงโมเลกุลของแบบจำลองที่สถานะปิดและสถานะเปิด ของแมกนีเซียมแทรนสพอร์เทอร์ในลิพิดไบเลเยอร์

นางสาวปัทมา วาปีสิทธิพันธ์

วิทยานิพนธ์นี้เป็นส่วนหนึ่งของการศึกษาตามหลักสูตรปริญญาวิทยาศาสตรมหาบัณฑิต
สาขาวิชาเคมี ภาควิชาเคมี
คณะวิทยาศาสตร์ จุฬาลงกรณ์มหาวิทยาลัย
ปีการศึกษา 2555

MOLECULAR DYNAMICS SIMULATION OF CLOSED AND OPEN STATE MODELS OF MAGNESIUM TRANSPORTER IN LIPID BILAYER

Miss Pattama Wapeesittipan

A Thesis Submitted in Partial Fulfillment of the Requirements
for the Degree of Master of Science Program in Chemistry
Department of Chemistry
Faculty of Science
Chulalongkorn University
Academic Year 2012

Thesis Title	MOLECULAR DYNAMICS SIMULATION OF CLOSED AND OPEN STATE MODELS OF MAGNESIUM TRANSPORTER IN LIPID BILAYER
By	Miss Pattama Wapeesittipan
Field of Study	Chemistry
Thesis Advisor	Associate Professor Pornthep Sompornpisut, Ph.D.
Thesis Co-advisor	Professor Supot Hannongbua, Dr. rer. nat.

Accepted by the Faculty of Science, Chulalongkorn University in Partial Fulfillment of the Requirements for the Master's Degree

.....Dean of the Faculty of Science
(Professor Supot Hannongbua, Dr. rer. nat.)

THESIS COMMITTEE

.....Chairman
(Assistant Professor Warinthorn Chavasiri, Ph.D.)

.....Thesis Advisor
(Associate Professor Pornthep Sompornpisut, Ph.D.)

.....Thesis Co-advisor
(Professor Supot Hannongbua, Dr. rer. nat.)

.....Examiner
(Assistant Professor Somsak Pianwanit, Ph.D.)

.....External Examiner
(Arthorn Loisruangsin, Ph.D.)

ปัทมา วาปีสิทธิพันธ์ : การจำลองพลวัตเชิงโมเลกุลของแบบจำลองที่สถานะปิดและสถานะเปิดของแมกนีเซียมแทรนสพอร์เทอร์ในลิพิดไบเลเยอร์. (MOLECULAR DYNAMICS SIMULATION OF CLOSED AND OPEN STATE MODELS OF MAGNESIUM TRANSPORTER IN LIPID BILAYER) อ.ที่ปรึกษาวิทยานิพนธ์หลัก : รศ.ดร. พรเทพ สมพรพิสุทธิ์, อ. ที่ปรึกษาวิทยานิพนธ์ร่วม: ศ.ดร. สุพจน์ หารหนองบัว, 61 หน้า.

แมกนีเซียมไอออน (Mg^{2+}) มีบทบาทสำคัญต่อกระบวนการทางชีววิทยา เช่น การสังเคราะห์ดีเอ็นเอและโปรตีน ปฏิกิริยาออกซิเดทีฟฟอสโฟรีเลชันและกระบวนการเมตาบอลิซึมด้วยเอ็นไซม์ แม้จะเป็นธาตุสำคัญและมีปริมาณมากในสิ่งมีชีวิต แต่ความรู้เกี่ยวกับกลไกการขนส่ง Mg^{2+} ยังมีไม่มากนัก CorA เป็นโปรตีนขนส่ง Mg^{2+} ที่สำคัญอันดับแรกของสิ่งมีชีวิตชนิดโพรแคริโอต โครงสร้างเอกซเรย์ของแมกนีเซียมแทรนสพอร์เทอร์ชนิด CorA จาก *Thermotoga maritima* วัดได้จากการทดลองที่มี Mg^{2+} สอดคล้องกับสถานะปิด อย่างไรก็ตาม คอนฟอร์เมชันที่สถานะเปิดยังขาดคำอธิบายที่ชัดเจน จึงจำกัดความรู้ความเข้าใจเกี่ยวกับกลไกการทำงานของการขนส่ง Mg^{2+} ในระบบชีววิทยา ในการศึกษานี้ได้จำลองคอนฟอร์เมชันที่สถานะเปิดโดยใช้ข้อมูลอิเลคตรอนพาราแมกเนติกส์เรโซแนนท์และกระบวนวิธี PaDSAR ตามด้วยการจำลองพลวัติเชิงโมเลกุล (MD) ของโครงสร้างในสถานะปิดและเปิดในลิพิดไบเลเยอร์เพื่อให้เข้าใจความสัมพันธ์ระหว่างโครงสร้างและการทำงานของโปรตีน แบบจำลองเชิงโครงสร้างของคอนฟอร์เมชันที่สถานะเปิดแสดงส่วนสทอล์คเฮลิกส์เคลื่อนเข้าใกล้แกนสมมาตรมากขึ้น ในขณะที่ส่วน TM1 เคลื่อนออกจากแกนหลักนี้ การจัดเรียงเชิงโครงสร้างดังกล่าวนำไปสู่การขยายโพรงในบริเวณเมมเบรน จากผลของ MD โดเมนเชิงโครงสร้างทั้งหมดของคอนฟอร์เมชันที่สถานะเปิดมีพลวัตสูงกว่าสถานะปิด ส่วนไซโตพลาสมิกโดเมนและเพอริพลาสมิกลูปมีความยืดหยุ่นสูงเมื่อเปรียบเทียบกับส่วนสทอล์คและแทรนสเมมเบรนเฮลิกส์ การวิเคราะห์โคออร์ดิเนชันของ Mg^{2+} ของบริเวณยึดจับทั้งหมดในการจำลองพลวัติเชิงโมเลกุลที่สถานะปิดพบว่า Mg^{2+} สร้างเฮกซะโคออร์ดิเนตกับลิแกนด์ที่ส่วนใหญ่มาจากเรสซิดิวซ์แอสปาร์เตตและ/หรือน้ำ กราฟโพรไฟล์ของแรงที่ใช้ในการเคลื่อนที่ของ Mg^{2+} ข้ามเมมเบรนโดยผ่านทางโพรงซึ่งวัดได้จากวิธีเสตียร์โมเลกูลาร์ไดนามิกส์แสดงค่าแรงขับดันที่สูงสำหรับการเคลื่อนที่ของ Mg^{2+} ที่บริเวณทางเข้าด้านเพอริพลาสมิกทั้งในสถานะปิดและเปิด ซึ่งชี้ในเห็นบทบาทที่เป็นไปได้ของเพอริพลาสมิกลูปสำหรับสมบัติการเป็นส่วนคัดกรองไอออน ข้อมูลจากการศึกษานี้ช่วยให้เข้าใจกลไกการขนส่งไอออนในโปรตีนขนส่ง Mg^{2+} ที่สำคัญอันดับแรกได้ดียิ่งขึ้น

ภาควิชา	เคมี	ลายมือชื่อนิสิต
สาขาวิชา	เคมี	ลายมือชื่อ อ.ที่ปรึกษาวิทยานิพนธ์หลัก
ปีการศึกษา	2555	ลายมือชื่อ อ.ที่ปรึกษาวิทยานิพนธ์ร่วม

5372284423 : MAJOR CHEMISTRY
KEYWORDS : MG^{2+} TRANSPORTER / CORA / MOLECULAR DYNAMICS SIMULATION / STEERED MOLECULAR DYNAMICS SIMULATION

PATTAMA WAPEESITTIPAN: MOLECULAR DYNAMICS SIMULATION OF CLOSED AND OPEN MODELS OF MAGNESIUM TRANSPORTER IN LIPID BILAYER. ADVISOR : ASSOC. PROF., PORNTHEP SOMPORNPISUT, Ph.D., CO-ADVISOR : PROF. SUPOT HANNONGBUA, DR. RER. NAT., 61 pp.

Magnesium ion (Mg^{2+}) plays a crucial role for biological processes such as DNA and protein synthesis, oxidative phosphorylation reaction and enzyme metabolism. Despite its biological abundance and importance, little is known about the transport mechanism of Mg^{2+}. CorA is the primary Mg^{2+} transport protein in prokaryotic organisms. The crystal structures of CorA from *Thermogota maritima* were determined in the presence of Mg^{2+}, corresponding to a closed state. However, the open state conformation has remained uncharacterized, thus limiting our understanding of the functional mechanism of Mg^{2+} transport in biological system. In this study, an open conformation has been constructed using electron paramagnetic resonance data and PaDSAR approach. Subsequently, molecular dynamics (MD) simulations of the closed and open conformations in lipid bilayer have been performed to understand the relation between structure and function of the protein. A structure model of the open conformation showed the stalk helices being closer to the symmetry axis while the TM1 helices move further away from the principal axis. Such structural arrangement has led to an increase of the pore cavity in the membrane region. From the MD results, all structural domains of the open conformation are more dynamics than those of the closed state. Within the protein, the cytoplasmic domain and the periplasmic loop are highly flexible with respect to the stalk and transmembrane helices. An analysis of Mg^{2+} coordination of all binding sites in the simulations of the closed conformation revealed hexa-coordinated Mg^{2+} with ligands mostly from either aspartate residues and/or water. The force profiles obtained from a steered molecular dynamics method showed a high driving force for the movement of Mg^{2+} at the periplasmic entrance of the pore in both closed and open states, suggesting a possible role of the periplasmic loop for the ion-selective property. The present study provided more understanding for the transport mechanism in the primary Mg^{2+} transport system.

Department : Chemistry Student's Signature .....
Field of Study : Chemistry Advisor's Signature .....
Academic Year : 2012 Co-advisor's Signature .....

ACKNOWLEDGEMENTS

I would like to express the deepest the appreciation to my advisor, Associate Professor Dr. Pornthep Sompornpisut, for his encouragement to do this research. He gave me a good opportunity to gain my experience of computational chemistry research. I also thank my co-advisor, Professor Dr. Supot Hannongbua for his useful advice and guide me to solve the research problems.

In addition, I am grateful to Associate Professor Dr. Vudhichai Parasuk who give a good advice for my research during the lab meeting of CCUC (computational chemistry unit cell) group. Special thanks for Dr. Viwat Vchirawongwin and Dr. Christopher Woods for teaching me about Perl and Python program which is very useful for my research. I would like to thank all member of CCUC for generous support and cheerfulness.

Finally, This work was fully supported by the Science achievement scholarship of Thailand, and the National Research University Project of CHE and Ratchadaphiseksomphot Endowment Fund (HR1155A) and the Thai Government Stimulus Package 2 (TKK2555) under the Project for Establishment of Comprehensive Center for Innovative Food, Health Products and Agriculture, as well as DPST scholarship from the Institute for the promotion of teaching Science and technology, Bangkok, Thailand.

CONTENTS

PAGE

LIST OF TABLES

LIST OF FIGURES

Page

Page

Page

LIST OF ABBREVIATIONS

3D	= Three dimension
Å	= Angstrom
Asn (N)	= Asparagine
Asp (D)	= Aspatic acid
DSSP	= Define Secondary Structure of Proteins
DCS	= Divalent cation sensor
EPR	= electron paramagnetic resonance
fs	= Femtosecond
Glu (E)	= Glutamic Acid
Gly (G)	= Glycine
His (H)	= Histidine
Ile (I)	= Isoleucine
L-J	= Lennard-Jones potential
MD	= Molecular Dynamics
ns	= Nanosecond
PaDSAR	= Pseudoatom-driven Solvent Accessibility Refinement
PB	= Poisson Boltzmann

PDB = Protein Data Bank

PME = Particle-mesh Ewald

POPC = Palmitoyl Oleoyl Phosphatidyl Cholines

RDF = Radial Distribution Functions

RMD = Restrained Molecular Dynamics

RMSD = Root Mean Square Deviation

RMSF = Root Mean Square Fluctuation

RNA = Ribonucleic acid

SMD = Steered Molecular Dynamics

TIP3P = Transferable intermolecular potential three -position

TM = Transmembrane

Tyr (Y) = Tyrosine

vdW = Van der Waals

VMD = Visual Molecular Dynamics

CHAPTER I
INTRODUCTION

1.1 Magnesium chemistry and prokaryotic magnesium transporter

Magnesium ion is present abundantly in living cells in the form of the divalent cation. The cellular concentration of Mg^{2+} in both eukaryotic and prokaryotic cells is about 15–25 mM. Mg^{2+} involved in many biological processes in cell system. For example, it plays as a cofactor with a great number of enzymes for a variety of physiological and biochemical processes including DNA/RNA transcription and replication, energy metabolism, protein translation, cell regulation, nerve and muscle functions.[1, 2] Interestingly, Magnesium ion has unique properties[3] compared to the other common biological cations including K^+, Na^+ and Ca^{2+}. For an example, the ionic radius of Mg^{2+} (0.86 Å) is the smallest of all cations, whereas its hydrated radius (2.09 Å) is the largest of all cations. Because Mg^{2+} has strong binding with water molecules, its hydration shell has slow exchange rate.[4] Thus, hydrated magnesium ion is more rigid than other ion. Mg^{2+} requires coordination number of 6 and an octahedral geometry. In contrast, Ca^{2+} has the flexibility structure and a greater range of coordination numbers. In crystal structure of protein, the distance between Mg^{2+} and oxygen atom of small molecule varies about 2.05 to 2.25 Å, whereas that of Ca^{2+} is wider and varies between 2.2 and 2.7 Å.[3] Due to the unique properties of Magnesium, it has imposed an interesting research subject for understanding the mechanism by which Mg^{2+} is transported across biological membrane. For example, how a transport protein specifically interacts and transports Mg^{2+} across the lipid bilayer? Whether Mg^{2+} is transported in the form of hydrated or bared cation? Up to now, the molecular mechanism of magnesium homeostasis is still unknown.

The transport of Mg^{2+} involves with a class of transport membrane proteins called magnesium transporter. There are three classes of Mg^{2+} transporters in Prokaryotic cell: CorA, MgtE, and MgtA/MgtB[5]. CorA and MgtE are found in Eubacteria and Archaea, while MgtA/MgtB is only found in the Eubacteria.[5-7] CorA contains a conserved GMN motif which appears to be the major Mg^{2+} uptake system. CorA has minimal sequence homology of Eukaryotic Mg^{2+} transporter, the Mrs2p

mitocondrail channel and the ALR protein of fungi.[8] The MgtA and MgtB Mg^{2+} transport system are P-type ATPases by sequence homology and regulated by PhoPQ system. All of bacterial magnesium transporters show the unique structures. CorA, named for the cobalt-resistant mutants, also transports Co^{2+} and Ni^{2+} ion.[9]

1.2 CorA Magnesium transporter

CorA is a primary Mg^{2+}transporter in most prokaryotes.[10] In 2006, the crystal structures of CorA Mg^{2+} transporter were determined from the thermophilic Gram-negative bacterium, *Thermogota maritima* by three researcher groups.[11-13] All crystal structures have the same general features corresponding to the closed state. CorA is cone-shaped homopentamer that can be considered as consisting of three major parts: inner and outer transmembrane segments (or TM1 and TM2), stalk helices and cytoplasmic domains. In membrane region, five TM1 and stalk helices formed the conductive pore.[10, 14] TM2 formed the outside concentric ring facing the hydrophobic lipid bilayer. TM1 and TM2 are connected by the periplasmic loop with highly conserved MPEL motif that was not resolved in crystal structure. Pro303 and Gly312 by the sequence YGMNF caused the distortion of TM1 near the periplasmic surface. At the C-terminus neat the end of TM2, the sequences of KKKKWL are located at the intracellular side arranging the basic sphincter. The distance of conductive pore starting from the periplasmic side to cytoplasmic side is about 40Å. There are three restrictions of pathway with ~6 Å and ~5.6 Å. The first constriction located at the periplasmic side is Asn314. The second is formed by Thr305 and Met302. At the interface between membrane and cytoplasm, Leu294 and Met291 formed the third constriction. The stalk helix linked to the N-terminal cytoplasmic which is a αβα sandwich consisting of two sets of α helices and seven-stranded parallel/anti-parallel β-sheet (Figure 1.1).

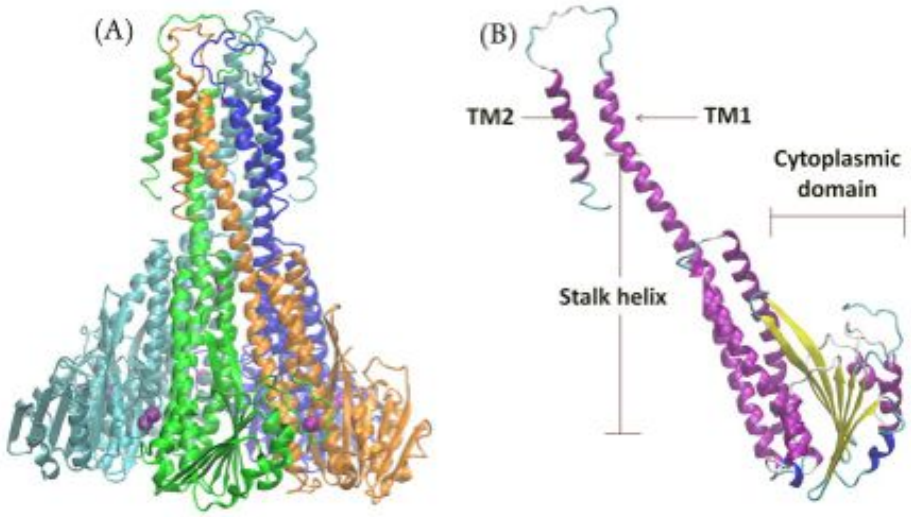

Figure 1.1 Schematic representation of (A) the pentamer structure and (B) the monomer structure of *T. maritima* CorA.[15] Three structure domains including transmembrane helices (TM1 and TM2), Stalk helix and cytoplasmic domains are illustrated.

Eshaghi et al. (2006) reported the 2.9 Å crystal structure of *T. maritima* CorA (PDB code: 2IUB).[11] The crystal structure has provided the structural framework for understanding the permeation and transport of Mg^{2+}. It has been proposed that the x-ray structure represents the closed state or non-conductive state because the pore of the CorA channel is identified as narrow and empty. The CorA structure which contains eleven Mg^{2+} bound to the protein has provided the two putative metal-binding sites (M1/M2) located at the interface between the N-terminal domains of pentamer. M1 is closely coordinated with the side chain of two acidic residues, Asp89 and Asp253 of the adjacent subunit. M2 near 7 Å from M1 is in cavity of the main chain of Leu12 and the side chain of Glu88, Asp175 and Asp253. The fact is that the protein was crystallized in presence of a high Mg^{2+}concentration. They suggest that the binding of Mg^{2+} in the M1/M2 binding sites could play an important role in regulating the CorA magnesium transporter. These M1/M2 binding sites have been hypothesized to act as a divalent cation sensor. At high intracellcular concentration of Mg^{2+}, ten Mg^{2+} were bound at these sites, giving rise to more intersubunit contacts which stabilize the CorA closed-state channel. The removal of Mg^{2+} in these sites allows movement of the CorA subunit which opens the CorA channel. From the CorA

crystal structure, one remaining Mg^{2+} is identified at the aspartic ring in the cytoplasmic pore. The role of this Mg^{2+} binding site is not yet understood.

In the same year, Payadeh et al. reported the CorA crystal structure (PDB code: 2NH2) at 3.7 Å resolution.[13] This structure has 12 divalent cations consisting of ten regulartory ions located at the interface between pentamer and two binding sites located in the conductive pore. One metal, which was observed around G309 at the conserved GMN motif, is stabilized within the transmembrane region. It might be the selectivity filter which discriminate between the size and preferred coordination geometry of hydrated cations.[13] The other binding cation is stabilized by D277 of two chains. They also identified ten metal-binding sites as term of a divalent cation sensor (DCS).[16]

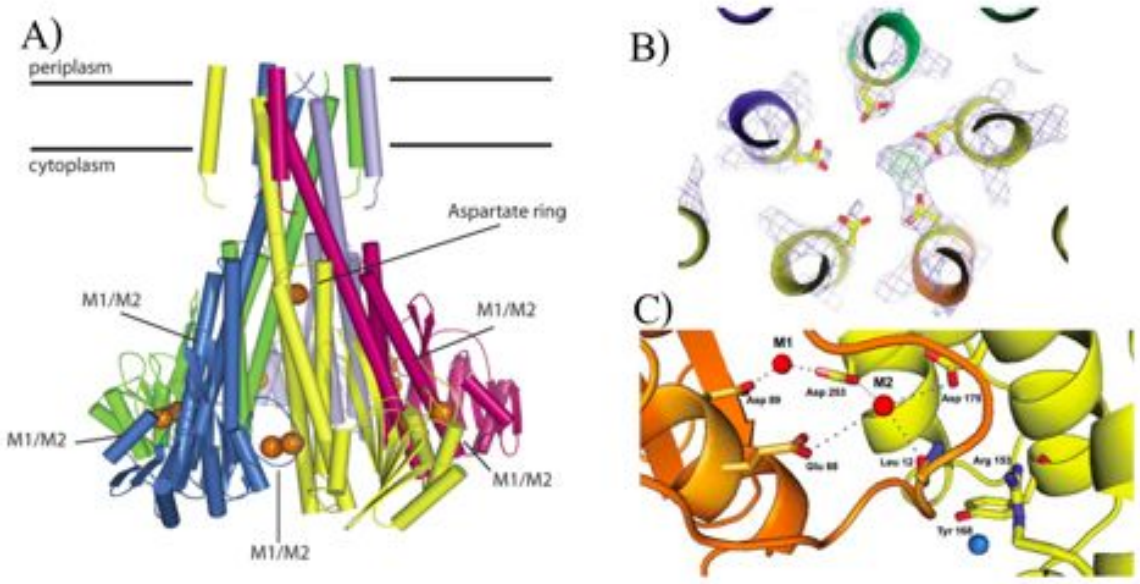

Figure 1.2 (A) The Mg^{2+} binding sites of the CorA crystal structure. Ten Mg^{2+} are identified at M1/M2 binding sites and one Mg^{2+} is located at the central pore. (B) The coordination of Mg^{2+} and aspartic sidechains showing the electron density of Mg^{2+} and its surrounding ligand atoms of carboxylate groups. (C) The metal-protein interactions in the M1/M2 binding sites.[11, 17]

1.3 Literature reviews of CorA Mg^{2+} transporter

In 2008, Payandeh and coworkers[18] studied the role of metal-binding sites for gating mechainism by using the site-directed mutagenesis of residues. They reported the three distinct regions might be involved the function of CorA. First, the divalent cation sensor (DCS) or M1/M2 site is proved to be involved in the regulation of the pore gating. It was found that the DCS induced the closed stated of CorA by forming the salt bridge of M1. Second, their results suggested that Pro303 and surrounding region is periplasmic gate of CorA. Third, Leu294, the narrowest constriction, is a hydrophobic gate (Fig 1.3). In addition, they mutated the acidic residues (E316 and E320) in highly conserved periplasmic loop (MPEL motif) and their data suggest that these highly conserved residues are not essential for selectivity filter but these acidic residues are electrostatic sink for concentrating cation near the periplasmic pore entrance. They also proposed TmCorA gating model as show in Fig1.3.

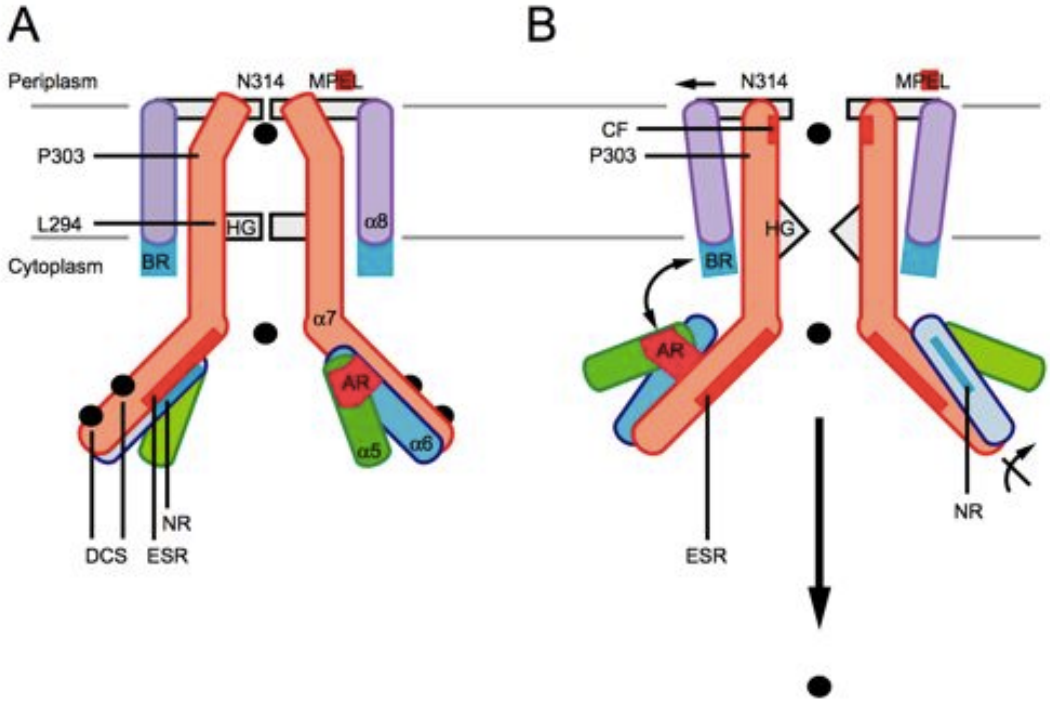

Fig 1.3 A proposed gating model of CorA illustrating the mode of TM1 and stalk helical motions from (A) a closed state to (B) an open state.[18] The permeation gate is near N314 and the hydrophobic gate is near L294.

Svidová et al. (2010) built three site-directed mutants at Leu294 position: Leu294Asp, Leu294Gly and Leu294Arg to confirm the importance of Leu294 for gating mechanism.[19] It was found that removing side chain (Leu294Gly mutant) or change to negative charge (Leu294Asp mutant) disturbed the regulation of Mg^{2+}.

Dalmas et al. (2010) used site-directed spin labeling (SDSL) and electron paramagnetic resonance (EPR) spectroscopy to investigate the mobility and structural dynamic of TmCorA in lipid bilayer.[15] The data shows the corresponding of the membrane conformation of TmCorA and the x-ray crystal structure. It was found that the transmembrane segments are the most dynamic region of the molecule. The modeling of conserved extracellular loops was refined based on EPR data combined with "Pseudoatom-Driven Solvent Accessibility Refinement" (PaDSAR)[20] method. In this refined loops model, the Glu316 moved forward to the center of the pore and contributed the electrostatic sink at the entrance of the pore (Fig 1.4). This model could accommodate the size and positive charge of the hydrated Mg^{2+}(Fig 1.4). It is possible that this loops act as "a selectivity filter".

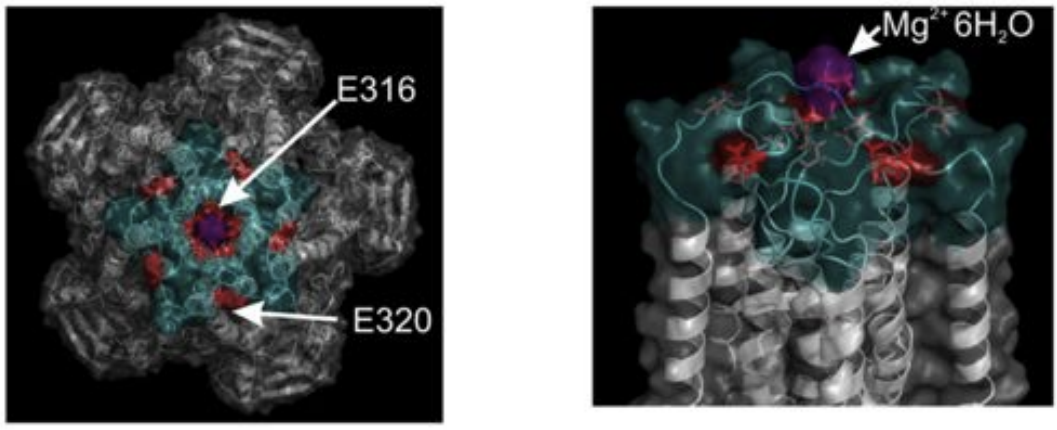

Fig 1.4 Top and side view of the refined loops model from PaDSAR method. A putative binding site contains Glu316 bound to hexahydrated Mg^{2+} represented by red and purple colors respectively.[15]

In 2010, Chakrabarti and coworkers performed molecular dynamics simulation of CorA in lipid bilayer with and without regulatory ions to investigate the influence of divalent cations on the molecular movements that allow to open the gate

of CorA.[21] From the simulation, they found that the absence of divalent cations in the putative regulation sites could trigger conformational changes of transmembrane helical bundle that possibly led to opening of the permeation pathway of the pore. In this study, they proposed a mechanistic model of an iris-like motion of pore dilation in the CorA magnesium translocation. This mechanism showed the wider pore by moving stalk helices to regulate the open form (Figure 1.5).

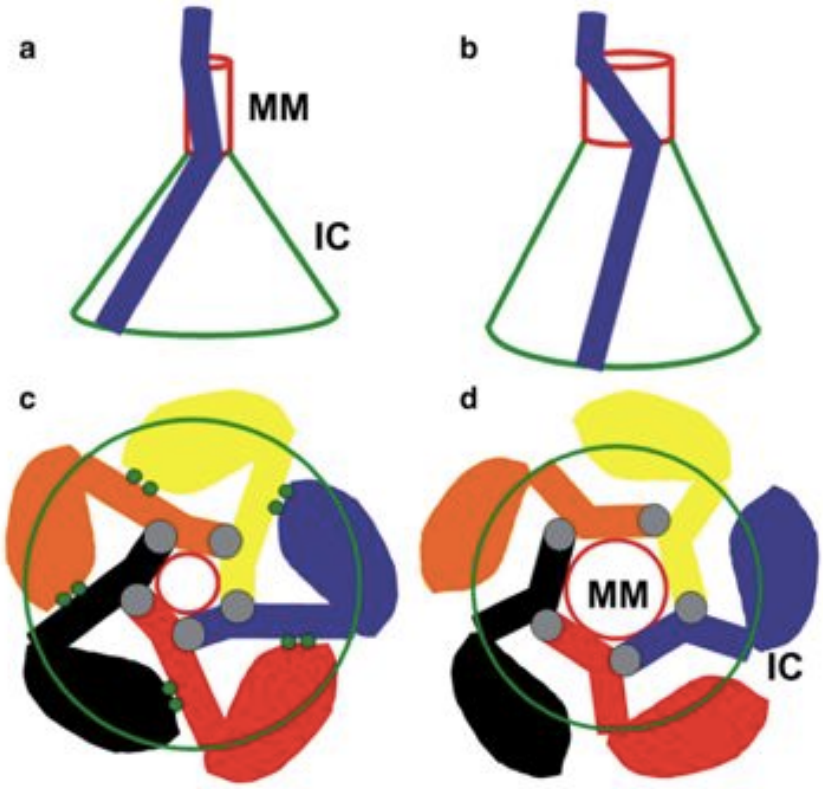

Fig 1.5 A proposed movement of stalk and TM1 helical bundle according to iris-like mechanism of pore dilation of CorA. (a) and (b) are top view, and (c) and (d) are side view. (a) and (c) are the closed state. (b) and (d) are the open state. [21]

The ion selectivity of CorA still remains unclear. This topic has been addressed by investigating the involvement of periplasmic conserved loop and selectivity cation in the extracellular region. In year 2009, Hu and colleagues have employed solution NMR technique to characterize the interaction between the transmembrane domain of CorA and its substrates (Mg^{2+} and Co^{2+}) as well as an inhibitor (hexaminecobalt(III)). They proposed that Mg^{2+} and hexaminecobalt(III)

binds to the same binding site which is located at the conserved periplasmic loop. They found the importance of glutamate residue in MPEL loop acting as an electrostatic ring for an interaction with divalent cations.[22] They also suggested "the cation binding is thought to be the hydrated state of Mg^{2+}". The fact is that hexaamminecobalt(III), the selective inhibitor, is the analog of hydrated form of Mg^{2+}.[23]. Therefore their result suggested that the fully hydrated Mg^{2+} initially interact with CorA. In 2010, Moomaw and Maguire[24] studied the mutation of charged residues in the loop of CorA. The results showed that there is no direct electrostatic interaction between Mg^{2+} and acidic loop residue. It also support that the loop is initial binding site of hydrated Mg^{2+}.

1.4 Molecular dynamics of biomolecules

Molecular modeling and simulation technique has become a powerful approach to investigate a variety of membrane-associated biological processes such as membrane protein oligomerization and assembly, transport across the membrane and membrane protein conformation changes upon activation.[25, 26] The technique such as molecular dynamics (MD) simulations has become a common approach to explore the relationship between structure, dynamics and function of protein in membrane environment at an atomic level.[27] The basis of MD simulation is relied on solving Newton's equation that determines the motion of individual particle as a function of time. Because of the advance computer power and the development of theoretical and algorithmic method, it is feasible to carry out MD simulation study of a large membrane protein system with all-atom representation. The result of simulation can be validated against spectroscopic data, e.g. NMR, EPR, fluorescense data. One should be noted that atomistic simulations are slow and could take several weeks or months per simulation. For investigating large scale motion such as channel gating, transmembrane domain motion, large-scale protein/lipid interactions, all-atom MD simulation may be limited by computing resources because these processes occur with time scale from microseconds to milliseconds as shown in Figure 1.6. [28]

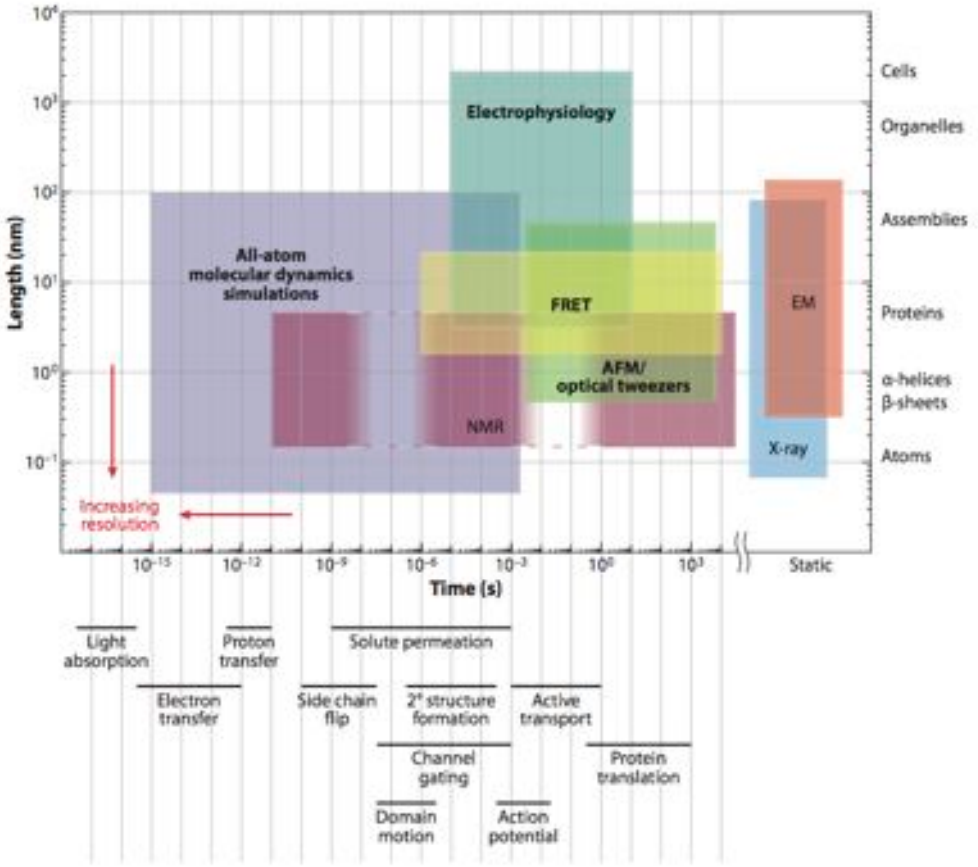

Figure 1.6 The time scale of the fundamental molecular processes and the composite physiological processes.[28]

1.5 Inspiration and objectives of this research

The study of Mg^{2+} translation in biological membrane could provide the fundamental basis for understanding Mg^{2+} permeation and transport. The molecular mechanism underlying the CorA magnesium transport requires detailed structure information of both the closed and open conformations of the protein. Unfortunately, all crystal structures of the CorA are only available for the closed state. The open state conformation remains uncharacterized. This study has been initiated with an inspiration of the extensive spectroscopic analysis by Dalmas et al. He and his colleagues have rigorously assessed the conformation of CorA reconstituted in bilayer under two different experimental conditions: with and without Mg^{2+}, by means of SDSL/EPR technique. They determined the spectral properties of both states for more

than a hundred of spin-labeled mutants. The study of mutated residues captures four regions: stalk, TM1, periplasmic loop and TM2, which are essential for demonstrating Mg^{2+} dependent conformational changes. The available experimental data taken from collaboration with this group allows a possibility to investigate an open conformation of CorA using PaDSAR, a specifically developed approach for modeling conformation changes of membrane protein using EPR restraints.

The main objectives of this study are:

1. To investigate structure and dynamic properties of closed and open state models of CorA by means of MD simulation
2. To evaluate the quality of the open-state model of CorA obtained from PaDSAR by means of MD simulation
3. To investigate Mg^{2+}coordination structure of individual metal coordination site in the closed state of CorA from MD trajectories
4. To investigate forces that required to translocate Mg^{2+} along the conduction pore of CorA in the closed and open-state models by means of steered MD simulation.

CHAPTER II
THEORY

2.1 Molecular dynamics

To perform MD simulation of biological macromolecule system, the initial coordinates and velocities of each atom in the system are needed. In order to calculate force acting on each particle, the classical equation of motion consisting of N particles (eq. 1) need to be solved.[29]

$$m_i \frac{d^2 r_i}{dt^2} = F_i = -\frac{\partial}{\partial r_i} U(r_1, r_2, \ldots, r_N) \quad \text{where } i = 1, \ldots, N \qquad (1)$$

This equation is 3N coupled second order differential equation. $U(r_1, r_2, \ldots, r_N)$ is the interatomic potential energy function which is consisting of bonded energy and non-bonded energy. In this research, the CHARMM force field was used in NAMD2 program.

2.2 Force field and the potential energy function for MD[30-32]

A force field is a mathematical expression describing the dependence of the energy of a system on the coordinates of the particles. The CHARMM potential function is shown in equation (2)

$$U = U_{bonded} + U_{non-bonded} \qquad (2)$$

The five terms are involved the bonded energy terms: the bonded stretching, angle bending, the dihedral term, improper term and the Urey-Bradley term.

$$U_{bonded} = \sum_{bonds} k_b (b - b_0)^2 \sum_{angles} k_\theta (\theta - \theta_0)^2 + \sum_{torsions} k_\phi [1 + \cos(n\phi - \delta)] + \sum_{improper} k_\omega (\omega - \omega_0)^2 + \sum_{Urey-Bradley\ terms} k_{UB} (u - u_0)^2 \qquad (3)$$

$k_b, k_\theta, k_\phi, k_\omega, k_{UB}$ refer to the force constant for bond stretching, angle, torsions anlge, improper bending and Urey-Bradley term respectively. The bond stretching term, the energy of a covalent between two atoms, is described by a simple harmonic

function. The second term is potential change upon the angle between two bonds. Torsions term is potential energy for the rotation of dihedral angles. Improper dihedral term is to preserve the geometry of four planar as shown in Figure 2.1. The Urey-Bradley is the energy cross terms described as a function of distance between the first and the third atoms.

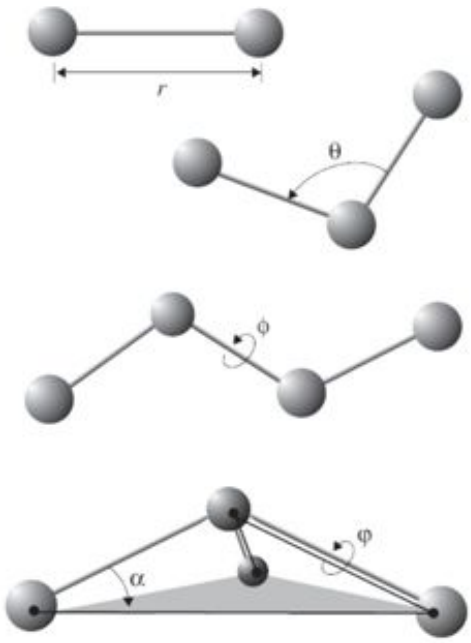

Fig 2.1 The force filed interactions: bond (r), angle (θ), dihedral angle (ϕ) and improper dihedral angle (φ).

$$U_{non-bonded} = \sum_{vdW} \epsilon \left(\frac{R_{ij}^{12}}{r_{ij}^{12}} - \frac{R_{ij}^{6}}{r_{ij}^{6}} \right) + \sum_{elec} \frac{q_i q_j}{r_{ij}} \qquad (4)$$

where R_{ij}^{12} and R_{ij}^{6} are coefficient and r is distance between the particles. $q_i q_j$ are partial charge of atom i and j.

The non-bonded energy is composed of van der Waals and electrostatic interactions as shown in equation (4). The van der Waals term known as the Lennard-Jones potential consists of an attractive and repulsive term. The repulsive interaction at short distance is due to the Pauli exclusion principle and the attractive force in longer distance is described by London dispersion. Calculation the Coulomb

electrostatic term is too computational costly, thus particle-mesh Ewald (PME) is needed to compute this term.

2.3 Integration algorithm

To solve the Newton's equation for MD simulation in equation (1), the integrator needs to calculate not only accurately but also efficiently for saving computation time. The velocity-Verlet algorithm is used for determining the positions of all atoms in trajectories.[33] According to Verlet algorithm, the equation of motion can be written by adding together of Taylor expansions of $r_i(t + \Delta t)$ and $r_i(t - \Delta t)$. The position and velocity of next time step can be calculated as follows:

$$r_i(t + \Delta t) = 2r_i(t) - r_i(t - \Delta t) + \frac{1}{m}F_i(t)(\Delta t)^2 \quad (5)$$

$$v_i(t) = \frac{r_i(t+\Delta t) - r_i(t-\Delta t)}{2\Delta t} \quad (6)$$

The modification of the Verlet algorithm is the leapfrog algorithm, written by

$$v_i\left(t + \frac{\Delta t}{2}\right) = v_i\left(t - \frac{\Delta t}{2}\right) + \frac{1}{m_i}F_i(t)\Delta t \quad (7)$$

$$r_i(t + \Delta t) = r_i(t) + v_i\left(t + \frac{\Delta t}{2}\right)\Delta t \quad (8)$$

2.4 NVT and NPT simulation

Biological system often is studied by the isothermal-isobaric ensemble (NPT ensemble) and the canonical ensemble (NVT ensemble) simulation. In constant temperature simulation, the classical equation of motion (eq. 1) is modified to Langevin equation by adding a friction force and a Gaussian noise term:

$$m_i\ddot{r}_i = F_i - m_i\Gamma_i\dot{r}_i + \xi_i(t) \quad (9)$$

where Γ_i is a friction constant and ξ_i is Gaussian noise. For NPT (constant temperature and pressure) simulation, the Legevin-Hoover's method is used[34]. The Langevin equation incorporates the constant pressure component of the Hoover equation, given by:

$$\dot{r}_i = \frac{P_i}{m_i} + \frac{p_{.psilon}}{W} r_i \quad (10)$$

$$.\dot{P}_i = -\nabla_{r_i}\Phi - \left(1 + \frac{d}{N_f}\right)\frac{p_{.psilon}}{W} P_i - \gamma P_i + R_i \quad (11)$$

$$\dot{v} = dvp_{.psilon}/W \quad (12)$$

$$\dot{p}_{.psilon} = dv(X - P_{ext}) + \frac{d}{N_f}\sum_{i=1}^{N}\frac{P_i^2}{m_i} - \gamma_p p_{.psilon} + R_p \quad (13)$$

The volume (v) is change via the motion of a piston, which control the pressure by coupling the system to a pressure bath (P_{ext}).

2.5 The Periodic boundary conditions (PBC)

PBC is the most popular choice of boundary condition to avoid the surface effects[33, 35]. All atoms in primary cell are replicated in all direction to form an infinite lattice of image cell. The image cell contains particles that are images of particle in primary cell (Fig2.1). When a particle moves out of the cell, its image particle will enter the cell at the opposite site. Because non-bonded interactions (Van Der Waals and electrostatic interactions) are calculated every pair of atoms including the image cell, it's impossible to calculate the long-range interactions. For PBC simulation, particle-mesh Ewald (PME) is used to compute the long-range interaction in order to reduce the computational cost. PME is described in the next section.

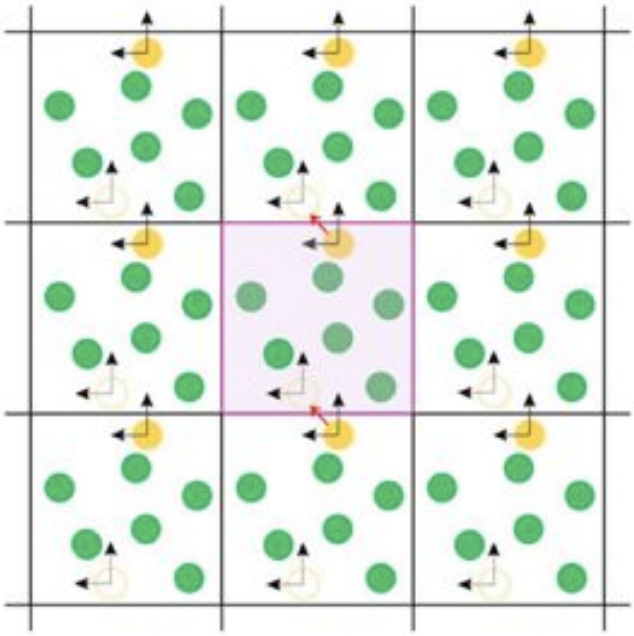

Fig 2.2 The simulation box of periodic boundary condition[33]

2.6 The Particle Mesh Ewald (PME)

PME method is fast numerical methods to treat electrostatic interactions of macromolecules system in periodic conditions.[35, 36] This method is based on interpolation of reciprocal space Ewald sums and evaluation of resulting convolutions using fast Fourier transforms.[32] The concept of PME is that Poisson equation can be solved much more efficiently if the charges are distributed in a mesh. Thus, the 3D-grid of particle mesh is created in the system over the distribution of the system charge. Then, the forces and potentials of atoms are determined from this charge. It's note that the grid size should be not too small in order to reproduce accurately charge distribution.

2.7 Steered Molecular Dynamics (SMD)

Steered Molecular Dynamics (SMD) is an MD simulation that applies an external force to biomolecules in a chosen direction. In SMD simulation, we can choose one or more atom to apply force. It's called SMD atom. The SMD atom is connected to a dummy atom with virtual spring. The external force is applied by

measuring from a harmonic potential and the dummy atom will move at constant velocity. The force depends on the distance between SMD atom and dummy atom. To setup the SMD, the spring constant should be high enough to ensure that it's closed to the potential in channel and not so high for making a noise. The force depends on the distance between SMD atom and dummy atom.

$$F = -\nabla U \tag{14}$$

$$U = \frac{1}{2}k[vt - (r - r_0) \cdot n]^2 \tag{15}$$

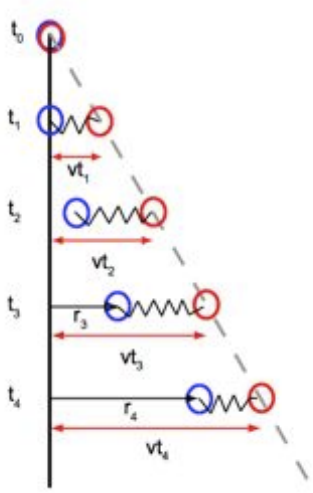

Fig 2.3 The virtual spring connecting between SMD atom and dummy atom

CHAPTER III
METHODOLOGY

3.1 Program

3.1.1 VMD (Visual Molecular Dynamics) [37]

VMD program is the interface program produced and developed by Theoretical and Computational Group in University of Illinois for displaying 3D structure and analyzing the MD results.[38] VMD program is a free program that is available on the Internet. (http://www.ks.uiuc.edu/Research/vmd/)

3.1.2 NAMD [39]

NAMD is the molecular dynamics software developed by the Theoretical Biophysics Group in the Beckman Institute for Advanced Science and Technology at the University of Illinois at Urbana-Champaign. To simulate the large biological macromolecule system, it was designed to run efficiently on parallel machines. NAMD require CHARMM force field.[40] (http://www.ks.uiuc.edu/Research/namd/)

3.1.3 HOLE

HOLE program was developed for visualizing and analyzing the pore radius of ion channel.[41] This program calculates the radius and represents the internal surface of the pore.

3.1.4 DSSP

The DSSP (Define Secondary Structure of Proteins) is an algorithm for assigning secondary structure information to amino acid of a protein[42].
(http://swift.cmbi.ru.nl/gv/dssp/)

3.1.5 Wordom

Wordom is a program for efficient analysis of molecular dynamics simulations. Wordom aims at fast manipulation and analysis of individual molecular structures and molecular conformation ensembles. The program is used to analyze secondary structure and distance analysis. Wordom is maintained and developed mainly in the Fanelli Lab at the University of Modena and Reggio Emilia (IT). The program is free software under the GPL license (http://wordom.sourceforge.net).

3.2 Modelisation of the open state of CorA model by PaDSAR

The open conformation of TmCorA was build starting from the closed state model from Dalmas's previous work[15]. The EPR experimental data of solvent accessibility and intersubunit distances were applied as structural restraint for restrained molecular dynamics, PaDSAR (pseudoatom driven solvent accessibility refinement)[20]. There are two sections of PaDSAR run for modelisation and validation of the TmCorA open structure. On the first PaDSAR run, the united-atom of protein model was conducted starting from closed state model using CHARMM PARAM19 force field. The spin-label pseudoatoms (Table 3.1) were attached to the alpha carbon of protein backbone on the basis of assignment from experimental O_2 and NiEDDA accessibility data (Figure 3.1). In the simulation system, there were the surrounding environment pesudoatoms (OXY and NIC) moving within restraint distance boundary. OXY and NIC could distribute within membrane region and aqueous phase respectively (Figure 3.2). During the simulation, the cytoplasmic domains were restrained on backbone atom. The stalk and TM1 helices of TmCorA were restrained by moving as a rigid body during the sampling. Because of losing the fivefold symmetry of the protein models, the individual monomer was replicated to form pentamer. Thereafter, distance restraint was used to validate the model candidates for selecting the best-fit models. The second PaDSAR run in the same protocol are performed again. The analysis of second PaDSAR run such as RMSD and HOLE plot was calculated for further validation. Finally, we selected the best model to perform MD simulation. Methodology for constructing the open-state model is summarized in Figure 3.3.

Table 3.1 Residue number of CorA with an assignment of the EP-types for open state modeling. The assignment was done by an analysis of ΠO_2, ΠNiEDDA and ΔH_o^{-1} profiles. All the pseudoatoms with the assigned EP-type were attached to the protein according to the method described in [43]. In the EPR dataset, some residues remained unassigned due to an ambiguity of the accessibility information.

Type*	**Residue number**
EP1	247 250 254 256 258 261 262 263 265 266 267 268 269 270 272 273 276 277 281 282 285 286 287 288 290 291 293 295 296 297 299 300 302 305 306 308 309 315 318 337 340 344 (n=42)
EP2	246 248 249 252 253 255 257 260 264 271 274 275 278 279 280 283 284 303 310 316 319 320 348 (n=23)
EP3	298 301 303 307 323 324 327 329 332 334 335 336 338 346 (n=14)
EP4	289 292 312 314 (n=4)

* EP1 = Buried, EP2 = Water-exposed, EP3 = Lipid-exposed, EP4= water-lipid interface

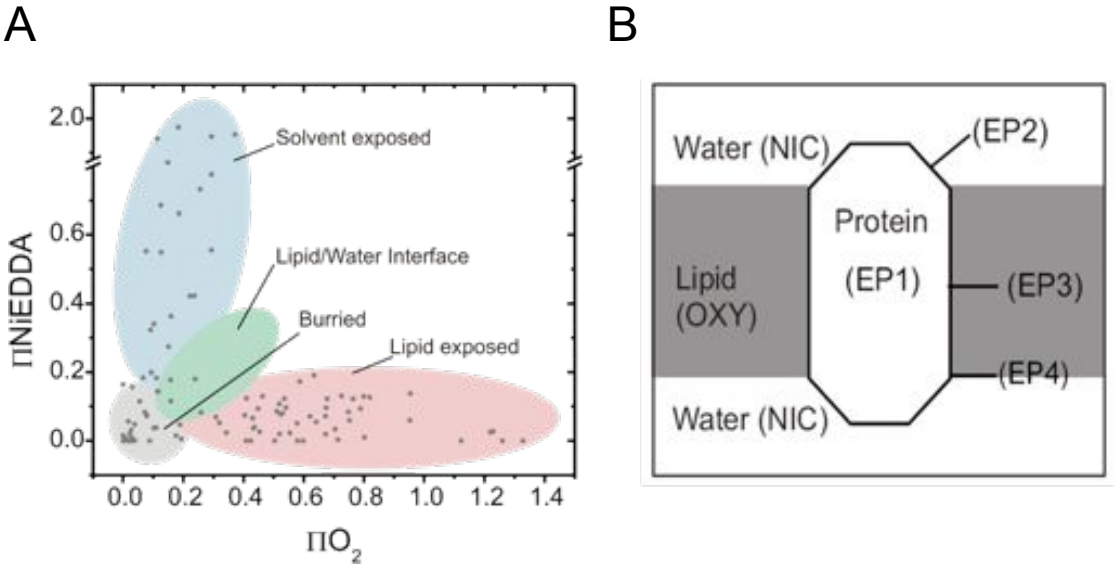

Figure 3.1 (A) An analysis of ΠO_2 versus ΠNiEDDA of the CorA open state (without Mg^{2+}) for the assignment of EP-type. The experimental ΠO_2 and ΠNiEDDA data have been given by Dalmas et al. (B) Schematic representation for definition of pseudoatoms used by PaDSAR.

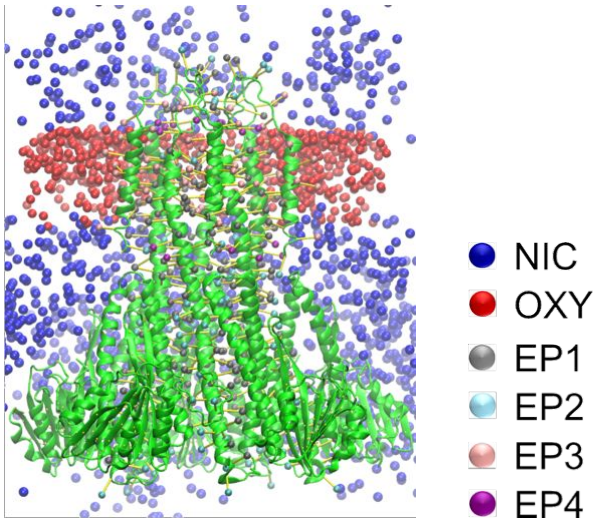

Figure 3.2 Modeling the CorA open-state conformation by PaDSAR. All pseudoatoms are shown as sphere.

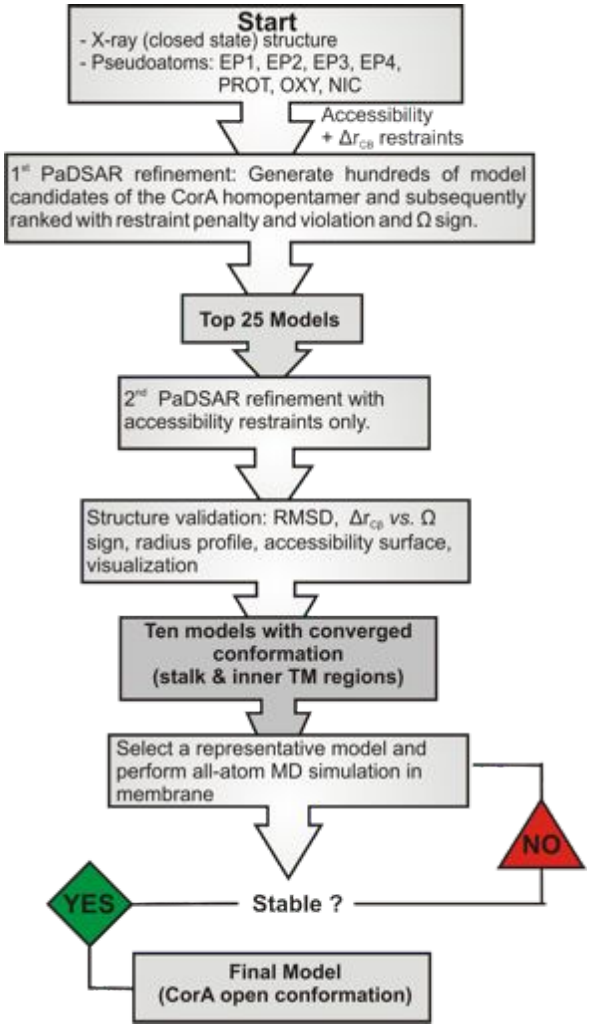

Figure 3.3 Flowchart of the PadSAR method used to generate structural models of CorA in its open conformation. The flowchart describes the iterative process used for modelisation.

3.3 Molecular dynamics simulations

To investigate the conformational stability of closed and open state of TmCorA, Two closed systems, which are different in the binding site of Mg^{2+} ions, and the open state model obtained from PaDSAR technique[20] are performed by means of MD simulations.

3.3.1 Preparing the simulation system

The x-ray crystal structure of TmCorA (PDB code: 2IUB) with modeling conserved periplasmic loops constructed by Dalmas research group was used in this

study[15]. Eshaghi's crystal structure revealed the one divalent cation binding site by D277 ring located at the permeation pathway, whereas the two divalent ion binding site formed by G309 and D277 are presented by Payadeh and Pai's crystal structure[13]. In this research, atomistic MD simulations of closed state CorA embedded POPC membrane were performed with the two different number of Mg^{2+} present in the metal binding sites of CorA. Closed I and Closed II denote, respectively, the simulation of 11 and 12 Mg^{2+} present in the binding site of CorA (Table 3.2).

Table 3.2 Summaries of Detailed Molecular Dynamics Simulations

Systems	Models	Number of Mg^{2+} ion	Number of solute atoms	Number of water atoms	Number of phospholipid atoms	Total number of atoms
Close I	Closed	11	28835	189819	66062	284876
Close II	Closed	12	28835	190836	65928	285752
Open	Open	-	28275	191454	64856	284800
SMD (closed)	Closed	1	28835	190362	66866	286225
SMD (open)	Open	1	28275	188982	65928	283397

All the protein models were inserted into a pre-equilibrated lipid bilayer, made up of ~480 molecules of 1-palmitoyl-2-oleoyl-sn-glycerol-3-phosphatidylcholine (POPC) embedded in ~64,000 TIP3P waters. Side-chain ionization states that were expected at pH 7 were assigned based on pK_a calculations using PROPKA. The pre-equilibrated patch of POPC membrane was built from VMD membrane builder plugin[37]. The protein was inserted into membrane patch by removing the lipid and water molecule that overlap with protein. The pore formed by TM domains of TmCorA was aligned with the z-axis of the membrane properly and placed at the center of lipid bilayer. To neutralize charge on the system, Na^+ and Cl^- ions were added randomly in the cytoplasmic bulk water by using VMD's Autoionize plugin. The final system of the Close I, Close II and Open contain approximately 290000 atoms (Table 3.2).

3.3.2 MD simulation protocol

To eliminate the high-energy contacts between protein and its surrounding, The systems underwent several energy minimizations and restrained MD steps. First, the systems were minimized for 5000 steps following by restrained MD steps with only relaxed lipid tail. After second energy minimization, MD steps were performed and harmonic restraints were imposed only on the protein. During restrained MD steps, forces were also applied to water molecules for prevention of hydration at the membrane hydrophobic region during equilibration. Lastly, free molecular dynamics were continued to further equilibrate the whole system.

All MD simulations were performed using NAMD2.7b program with full electrostatics using particle mesh Ewald and periodic boundary condition using the CHARMM22 and CHARMM27 force fields for protein and lipid molecules respectively. For water, the TIP3P models of water were used. The NPT ensemble was used to perform MD simulation in 1 atm and 300 K. The simulation temperature and pressure were kept constant by using Langevin dynamics (LD) and Nośe-Hoove Langevin Piston respectively. An integration time steps of 2 fs were employed with the SHAKE algorithm to fix all bonds involving hydrogen atom. The configurations and velocities were stored every 2 ps. Each system was carried out in the MD simulations more than 100 ns.

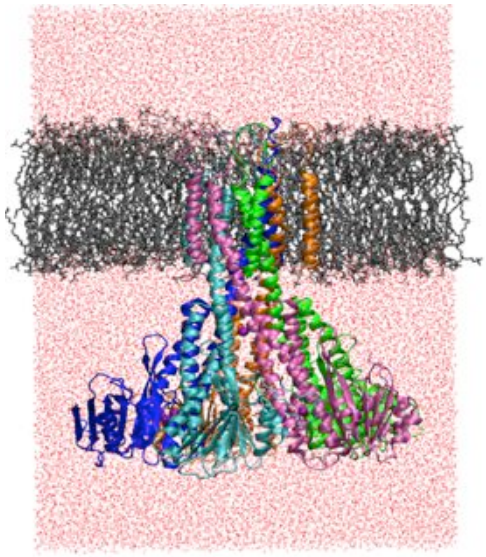

Figure 3.4 The box simulation of CorA Mg^{2+} transporter in POPC lipid bilayer.

3.4 Analysis tool of MD trajectories

During MD simulation, the velocities and coordinates of the atom in time were collected in term of trajectories. VMD program is used to visual trajectories from MD simulation. To address the problem, MD trajectories can be analyzed in several ways depending on the object of the investigation. For an example, RMSD is normally used to define the reach of thermodynamic equilibrium of the system. At equilibrium, RMSD value is reach to steady value. In this study, the computation of RMSD is to monitor the stability of the protein. RMSD of the protein can be calculated the difference between two structures. The flexible of the protein were obtained from RMSF of each residue. Pore radius profiles were calculated using HOLE[41]. Secondary structure analysis used DSSP algorithm.

3.5 Steered Molecular Dynamics Simulation

Steered molecular dynamics simulation (SMD) was performed on two model systems: the closed and open state conformations (Table 3.2). CHARMM22 and CHARMM27 force fields were used for protein, lipid, water and Mg^{2+}. The starting models were the x-ray structure for the closed state and PaDSAR structure for the open state. The Mg^{2+} ion was initially placed at the extracellular side near the entry mouth of the pore (Figure 3.5). Then, the closed state and open state of TmCorA embedded the hydrated POPC bilayer were prepared and minimized by using the same method as described in MD section. After 2 ns of equilibration with Mg^{2+} constraint at initial position, the steered molecular dynamics (SMD) were conducted for transmembrane channel starting from the periplasmic entrance (z = 20 Å) to the cytoplasm (z = -40 Å). A harmonic constraint of 5 kcal/mol $Å^2$ was applied to Mg^{2+} ion in the z-direction along the pore with a constant velocity (0.01 Å/ps). An integration time steps of 1 fs was used. The trajectories were generated for every 1 ps. NAMD2 program was used for performing SMD simulation.

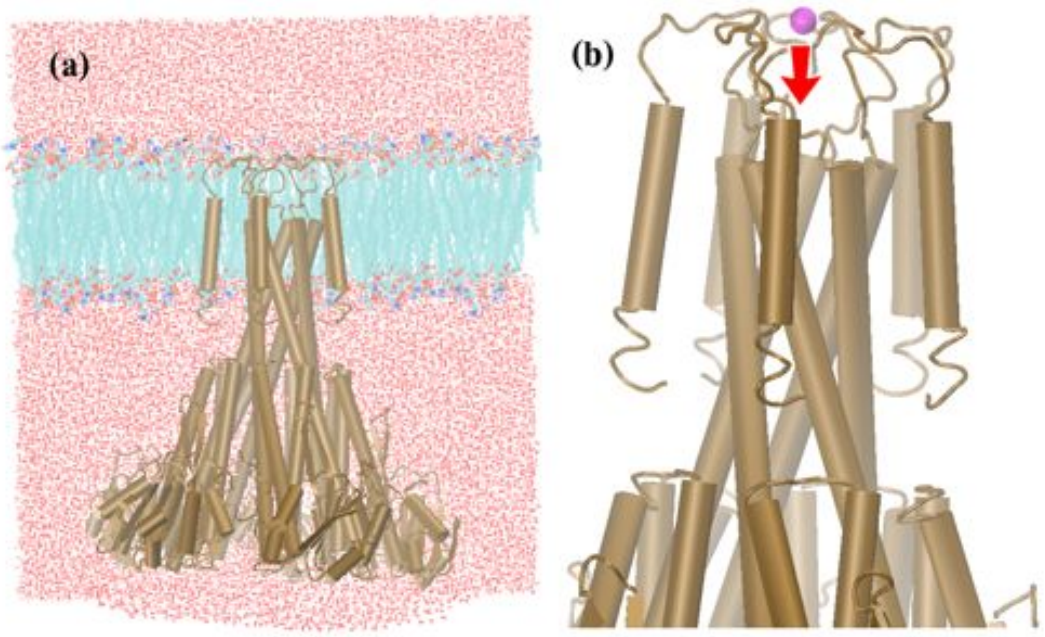

Figure 3.5 (a) Simulation box of SMD. (b) Initial position of Mg^{2+} and direction of forced applied to Mg2+ to translocate along the conduction pore of CorA

CHAPTER IV
RESULTS AND DISCUSSION

4.1 Open model of CorA

The present EPR dataset together with structure modeling approach allow one to construct an open-state conformation of CorA. The RMSD value calculated for the backbone atoms of the ten best structures is 2.12±0.54Å. This value is in a generally accepted measure for the quality of calculated structures. From the superimposed structures within the ensemble (Figure 4.1), stalk and TM1 helices showed well-defined regions with RMSD of 1.68±0.42Å whereas the cytoplasmic domain and the periplasmic loop were poorly defined with RMSD of 5.98±2.56 and 6.94±2.0Å, respectively. For TM2 helix, RMSD calculated over the ensemble of ten structures was 2.75±1.10Å. It should be noted that the RMSD values were computed based on a structure alignment of the stalk, TM1 and TM2 helices. These superimposed regions provide experimental data for EPR restraints and their secondary structures were maintained during PaDSAR calculation.

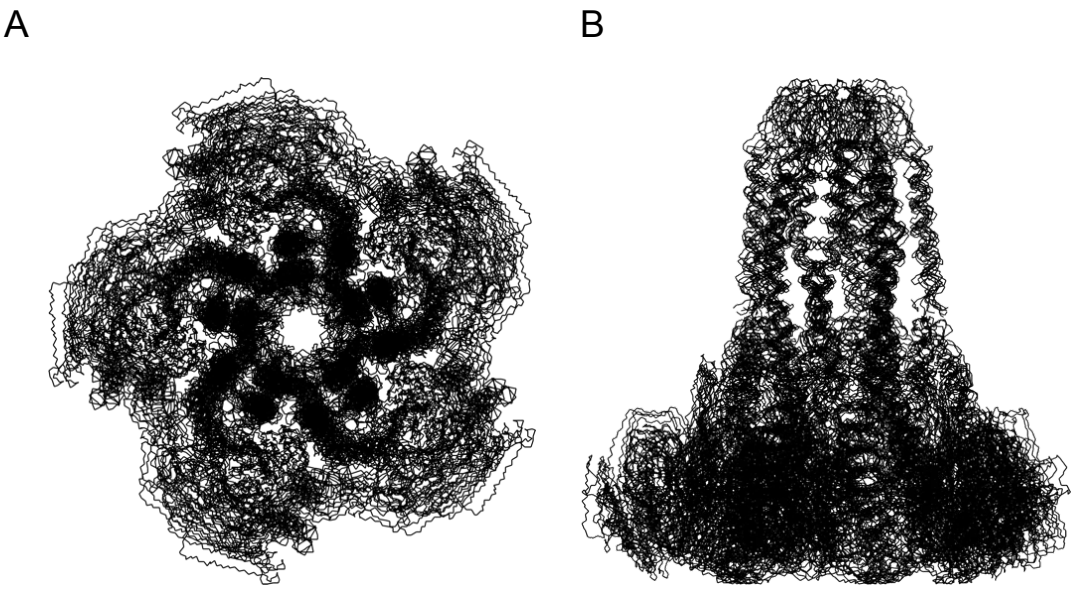

Figure 4.1 An ensemble of ten structures of the open-state model of CorA: (A) top view and (B) side view

Inspecting the difference in the diameter of the pore between the closed and open conformations provides useful insight into Mg^{2+} transport in CorA (Figure 4.2). In the closed conformation, the pore that is formed by the arrangement of stalk, TM1 and periplasmic loop of five subunits can be described as a long and narrow permeation pathway. The diameter profile of the closed conformation illustrates several narrow constrictions with a diameter of 2-3Å. Residues that constitute narrowly constricted pore are Met291, Leu294 Met302, Thr305, Met313 and Glu316. Apparently, these residues are located in TM1 (Met291, Leu294 Met302, Thr305) and the periplasmic loop (Met313 and Glu316). The open conformation showed an expansion of many constriction sites that made the wider pore being large enough for a passage of the Mg^{2+} in the hexa-hydrated form. An increase of the pore-size cavity in the membrane region can be described by structural rearrangement of transmembrane helical bundle associated with the movement of stalk helix. Such conformational rearrangement results in weaker helical contacts among the five monomers of CorA. This result is strongly supported by an increase of experimental mobility for the inner transmembrane segment.

It should be however noted that the pore size in the open conformation by taking into account structure deviation (error bars) contains putative constriction region around the periplasmic loop and near Met313, Glu316 and Met318. The presence of the putative constriction sites in the open conformation is likely to control Mg^{2+} translocation across the permeation pathway by the ion-selective property. The presence of ion-constriction can explain an inhibitory effect of CorA magnesium transporter by hexamminecobalt(III) channel blocker, an analog of hydrated Mg^{2+}. In the next section, a study of molecular dynamics simulation has illustrated a role of the periplasmic loop on the ion-permeation gate.

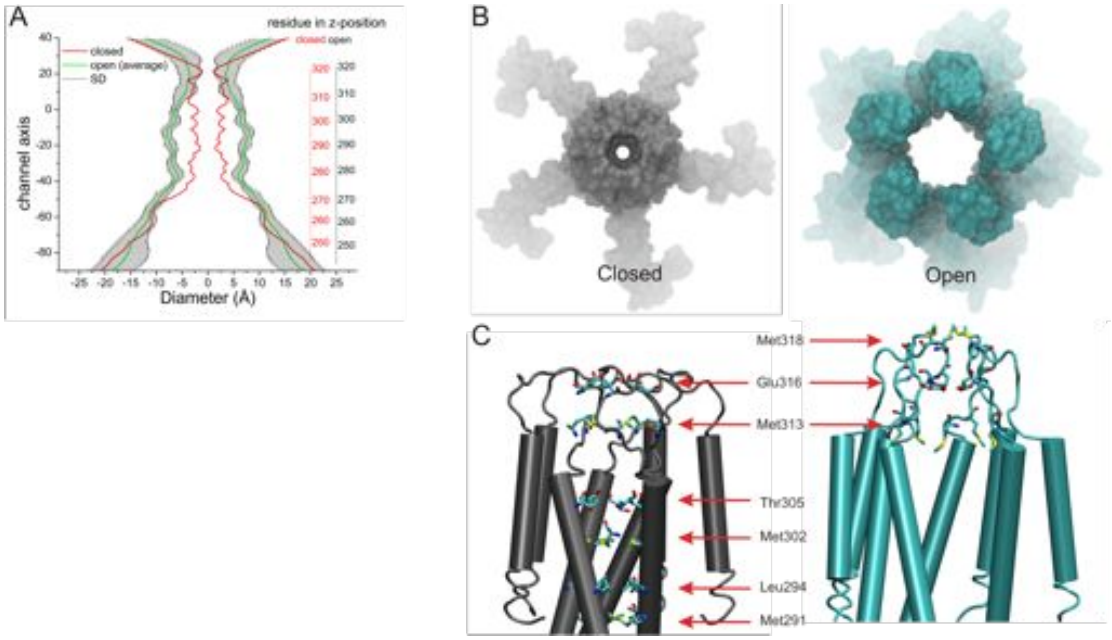

Figure 4.2 (A) Graphical presentation of pore diameter profiles of the closed (red line) and the open conformation (green line)**.** The diameter profile of the open model with standard deviation (error bars) is an average value obtained from the ten models. (B) Channel interior represented by molecular surface of the stalk+TM1 helix. (C) Residues facing toward the pore and forming narrow constriction sites.

Structure model of CorA in its open conformation revealed plausible structural insight into conformational changes underlying a structural transition between the closed and open states in CorA (Figure 4.3). Upon gate opening, the stalk helices move closer to the symmetry axis while the TM1 helices move further away from the axis. Superimpose of the closed and open conformations revealed Gly274 may serve as a pivot point for a kink between the stalk and TM1 helix. Considering the rigid-body movement of stalk and TM1 helix together with the presence of the kink, molecular mechanism of CorA gating corresponds to scissor-like motion. As the results, the inner cavity that contains the hydrophobic constriction pore in the membrane becomes wider and expands the permeation pathway.

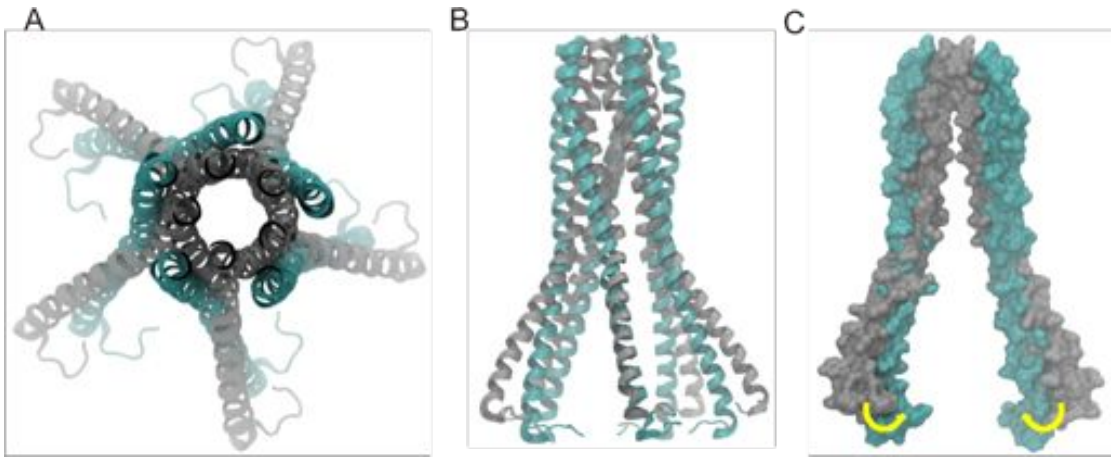

Figure 4.3 Conformational rearrangement upon structural transition between the closed (gray) and open (cyan) states in (A) top view and (B) side view. (C) Molecular surface representation illustrates a scissor-like motion of stalk+TM1 helix upon gate opening of CorA transporter. The figure is showing only two subunits of stalk+TM1 helix of CorA for clarification.

4.2 The structural stabilities of the protein

After the MD simulations had been complete, the dynamic trajectories for the system are produced. The average structural properties of the system were analyzed based on the dynamic trajectories. The RMSD profile of the simulation showed stability of the protein. Production run of the simulations was analyzed to examine dynamics properties of the simulated systems. According to Figure 4.4, The RMSDs of the two closed and open system versus the simulation time correspond to different domains of protein and different chains that are presented. Due to the restrain on backbone of the protein during the first 6 ns, the values of RMSD are low and then climb sharply and reach to small fluctuation without any restrains. This implies that the structures of protein have a slight change in conformation and stable in POPC membrane during the simulation. Analysis of RMSD as a function of time shows the equilibrium of the system

An analysis of structural stabilities and dynamics were carried out with four different regions: stalk and inner transmembrane helices (TM1), outer transmembrane helices (TM2) and cytoplasmic domains. The RMSD profiles calculated for the backbone atoms of the Close I, Close II and Open systems are similar in a way that

the cytoplasmic domains exhibit the most mobile region in the protein (Figure 4.4). One can see that the RMSD profiles of the stalk+TM1 and TM2 are similar between Close I and Close II (Figure 4.4A and 4.4B). The fluctuation of RMSD values of two transmembrane helices (the green and blue lines) are smaller than those of the cytoplasmic domains indicating that TM1 and TM2 undergo small structure changes with respect to that of the cytoplasmic domain. It is likely that the simulation of Close II showed the protein with the greatest structural stability (Figure 4.4B). This result suggested that the presence of Mg^{2+} bound in the periplasmic loop influences structural stability of the protein. This finding is in good agreement with experimental study of previous reports. It has been shown that the periplasmic loop contains the conserved MPEL residue and the GMN motifs that may act as the ion-selective filter. It appears that the selective binding site of Mg^{2+}, possibly the negatively charged glutamate residue near the extracellular mount of the pore, stabilizes the oligomeric state of the CorA channel. The hypothesis of ion stabilization in the pore is supported by an apparent increase of the RMSD profile of the stalk+TM1 helix in the open-state simulation. RMSD of individual monomer showed that Close II systems exhibited a small fluctuation of the stalk+TM1 helix in a range of 1 to 3 Å. However, the simulation of the free Mg^{2+}-bound CorA in its open conformation illustrated a relatively large RMSD value compared to Close I and Close II as shown in Figure 4.4 (right). The observed results are in good agreement with the role of the metal-binding site at the periplasmic loop on symmetric stability in protein pentamer. From the simulation of the open conformation, it has been found that one of the homopentamer showed a distinct RMSD shift for the stalk+TM1 helix compared to the rest four subunits. This implies that MD simulation with the absence of Mg^{2+} revealed a tendency to lose structural symmetry in CorA. The results of this study support the crystallographic study of TmCorA mutants described previously. It was found that an asymmetric conformation in CorA has been observed from crystal structures of truncated N-terminal TmCorA mutant obtained with and without divalent cations. In the Mg^{2+}-bound mutant, one of the five GMN motifs did not directly coordinate to the metal ion, and thus was observed as a disordered chain. The asymmetric arrangement has become more apparent in the case of x-ray structure of TmCorA mutant without Mg^{2+}. It should, however, be noted that the mechanism of asymmetric structural

transition is not complied with a concerted motion of the CorA gating model reported previously.

The simulation of the open state conformation exhibited distinct RMSD values compared to those of the closed conformation. For open state system, the average RMSDs of stalk helices and outer transmembrane helices are 4 Å and 6 Å respectively. The cytoplasmic domain has the largest RMSD around 8 Å with respect to the starting structure. It has been found that the secondary structure contents of the cytoplasmic domain did not deform during the course of MD simulation. This suggested that the whole domain motion likely took place during channel gating. However, the present dataset are available for protein starting the stalk region. Thus it is insufficient to discuss such domain motion observed from the simulation due to the lack of structure information on the cytoplamic domain. The only explanation is structural relaxation to accommodate the structure changes of the stalk and TM1 helix in the open model. An analysis of the outer transmembrane helices showed structural stability as indicated by the smallest RMSD values. Analysis of RMSD as a function of time shows the equilibrium of the system before the end of simulation. The production phase can be considered after 50 ns. Thus, the trajectories of after 50 ns are extracted for further analysis.

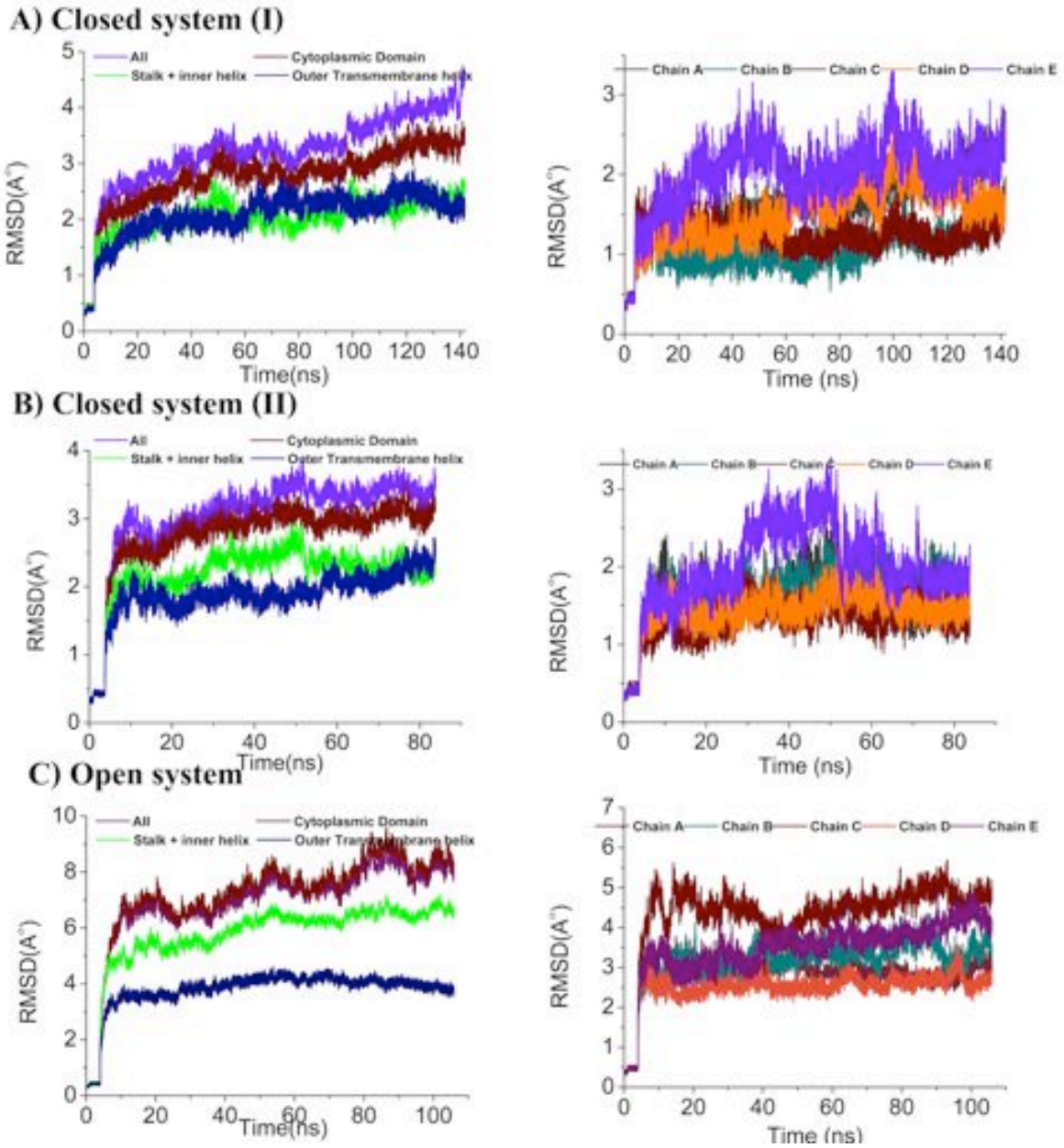

Figure 4.4 RMSD profiles versus simulation time of Closed I (A), Close II (B) and the open state (C) of CorA. Left and right graphs illustrate RMSD of five monomer and of the stalk+TM1 residues of monomer, respectively.

Monitoring protein dynamics from the simulations have been achieved by computing root mean square fluctuations (RMSF), an analysis of structure fluctuation with respect to the average structure. Figure 4.5 illustrates RMSF for individual residue of the protein measured using the last 10 ns of the trajectories. RMSF profiles of the simulations of Close I and Close II were slightly different, suggesting that the

presence and absence of Mg^{2+} in the periplasmic loop did not significantly alter global dynamics of the protein in the closed conformation. However, the open conformation of CorA is globally more dynamics as evidence of greater RMSF values for almost every positions of the protein compared to those of the two closed-state simulations. This result led to the conclusion that the arrangement of five monomeric subunits of CorA in its closed conformation is more compact than that of the open CorA. It is anticipated that in order to regulate CorA gating, the cytoplasmic, stalk and transmembrane domains would become more dynamics as a structural transition to expand the permeation pathway. A comparison of residue-based RMSF of residues encompassing 250 to 349 led to conclude that stalk and transmembrane helices behave as rigid bodies whereas the extracellular periplasmic loop are likely disordered and mobile. To compare between two transmembrane helices' RMSF, TM2 is more flexible than TM1. The RMSF range of cytoplasmic region (residues 6 to 244) is about 0.5 to 1.5.

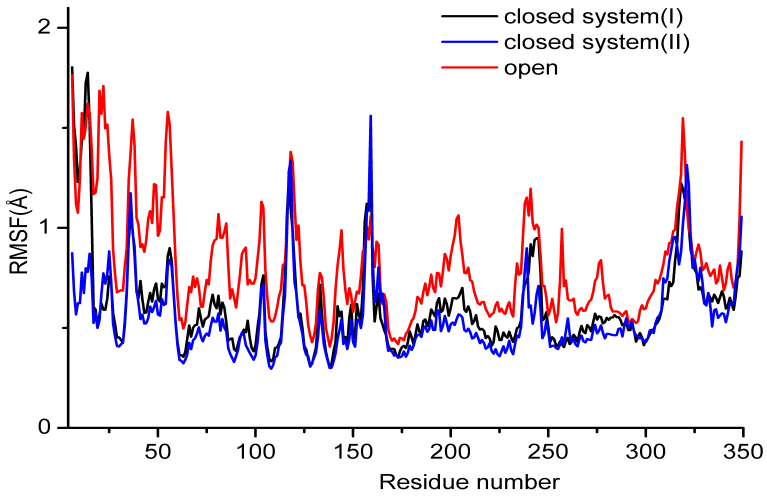

Fig 4.5 Average backbone RMSF of closed system (I)(black), closed system (II)(blue) and open system (red)

Furthermore, backbones RMSF of each subunit for Close I, Close II and Open systems were also calculated (Figure 4.6, 4.7 and 4.8). Due to the same structure of individual subunit, RMSFs of each subunit have overall the same pattern depending on the secondary structure of monomer.

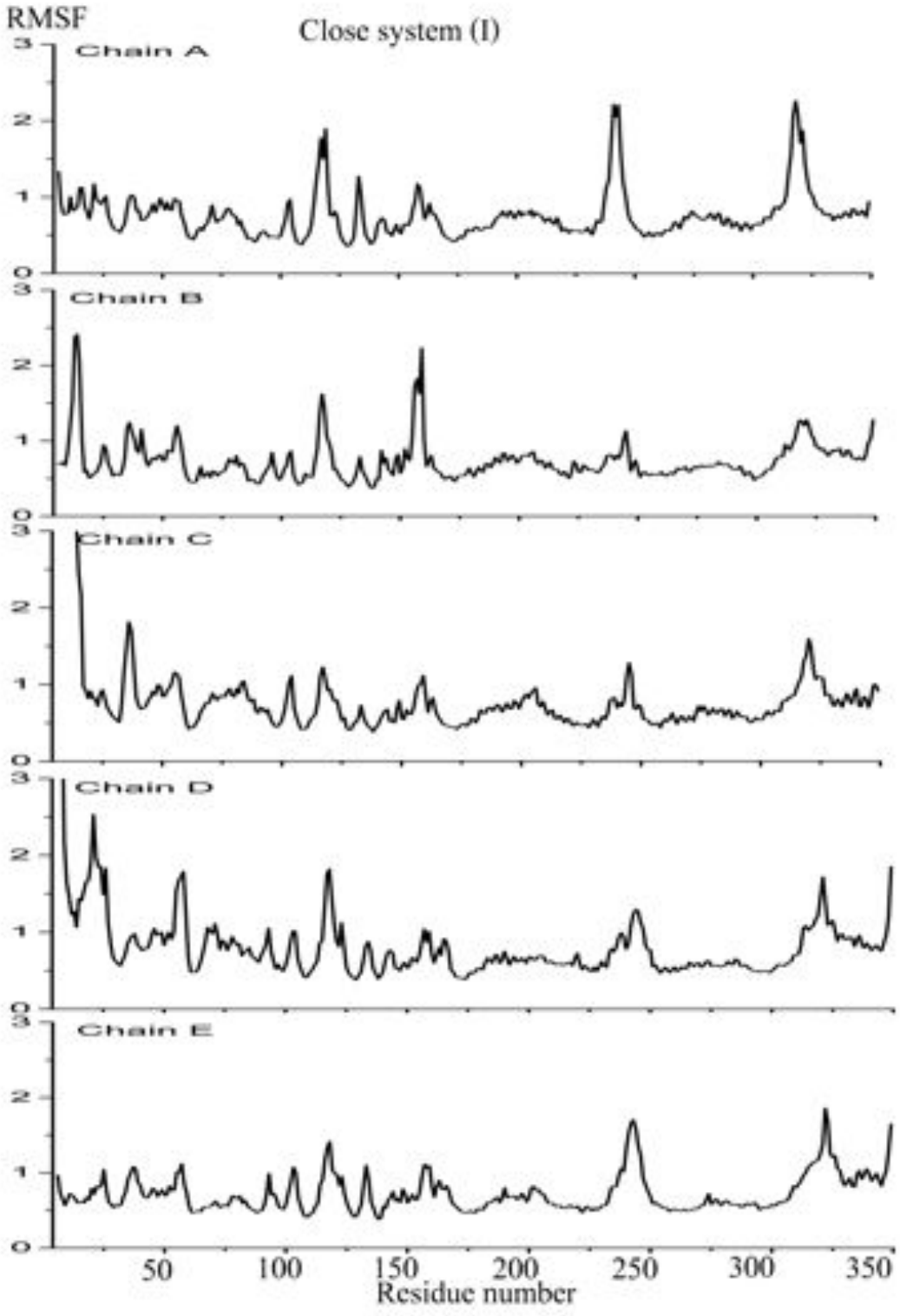

Figure 4.6 Backbone RMSF as a function of residue number of close (I)

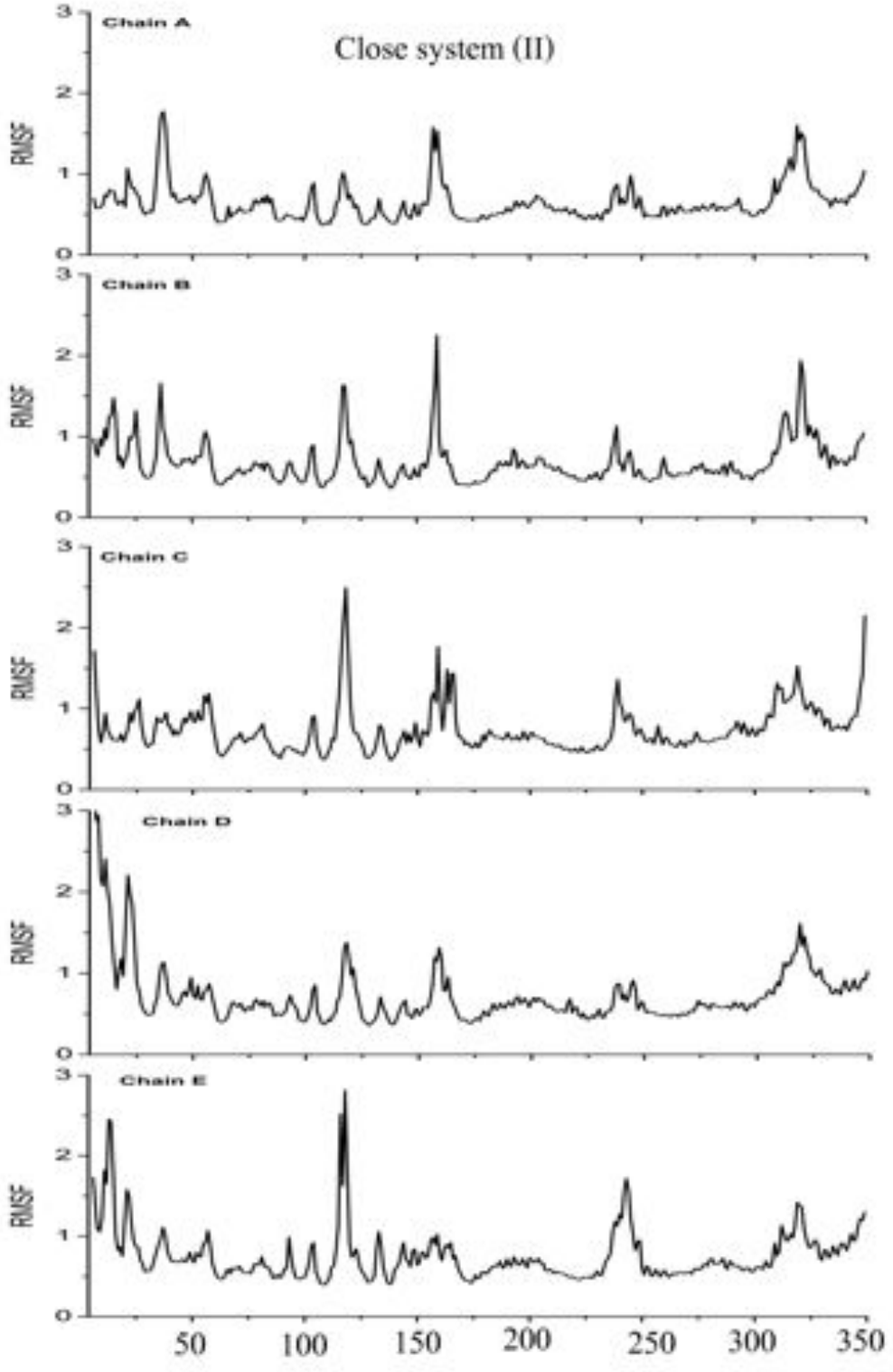

Figure 4.7 Backbone RMSF as a function of residue number of close (II)

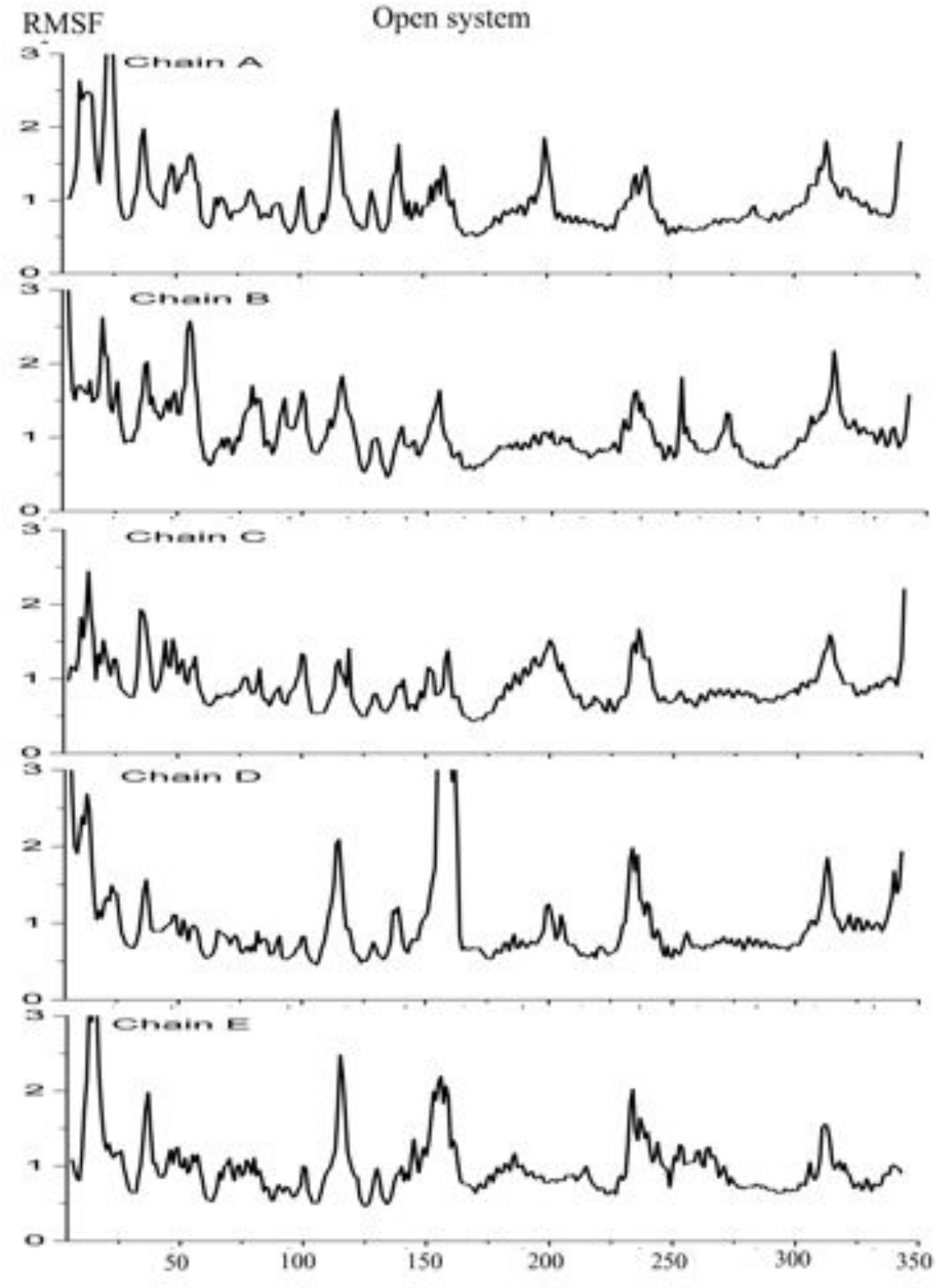

Figure 4.8 Backbone RMSF as a function of residue number of open system

The RMSF of pentamer for each domain: TM1, TM2, stalk helix and loop are represented by statistical box and whisker diagram as shown in Figure 4.9. The bottom and the top of the box are 25 and 75 percentile. The median is the straight line, and the mean is plotted as a square. A comparison between the RMSF data and the experimental mobility parameter (ΔH_0^{-1}) obtained from SDLS/EPR technique with and without intracellular Mg^{2+} (data not shown) revealed considerable consistency. The open conformation is in overall more mobile than the closed conformation, except for the loop. The overall trend of both data shows the higher mobility of open state especially the inner transmembrane (TM1). This may be taken as evidence that the TM1 of open state is mobile for gating mechanism. From the experiment, TM2 has the most dynamic while the RMSF from simulation periplasmic loop has the most flexible. The stalk elements of both data are the most static structure.

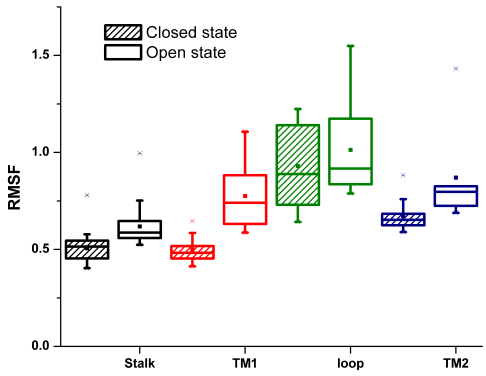

Fig 4.9 Box plot of RMSF of closed and open state of CorA.

To verify a stability of secondary structure, secondary structure of protein as a function of time can be assigned using DSSP (Figure 4.10, 4.11 and 4.12). In the closed state system, α-helical conformation of the protein (red color region) remains significantly unchanged during the course of the simulation. It indicates that the stalk and transmembrane helices were stable over the simulation time. Other main secondary structure elements are also conserved throughout the simulation such as beta sheet in the cytoplasmic domain (blue region). The overall secondary profile of open state, as shown in Figure 4.12, shows the same pattern with that of closed state. Nevertheless, some transient changes in secondary structure of open state are

recognized but not significant. From these results, it is concluded that CorA undergoes rigid body motion between the closed and open states.

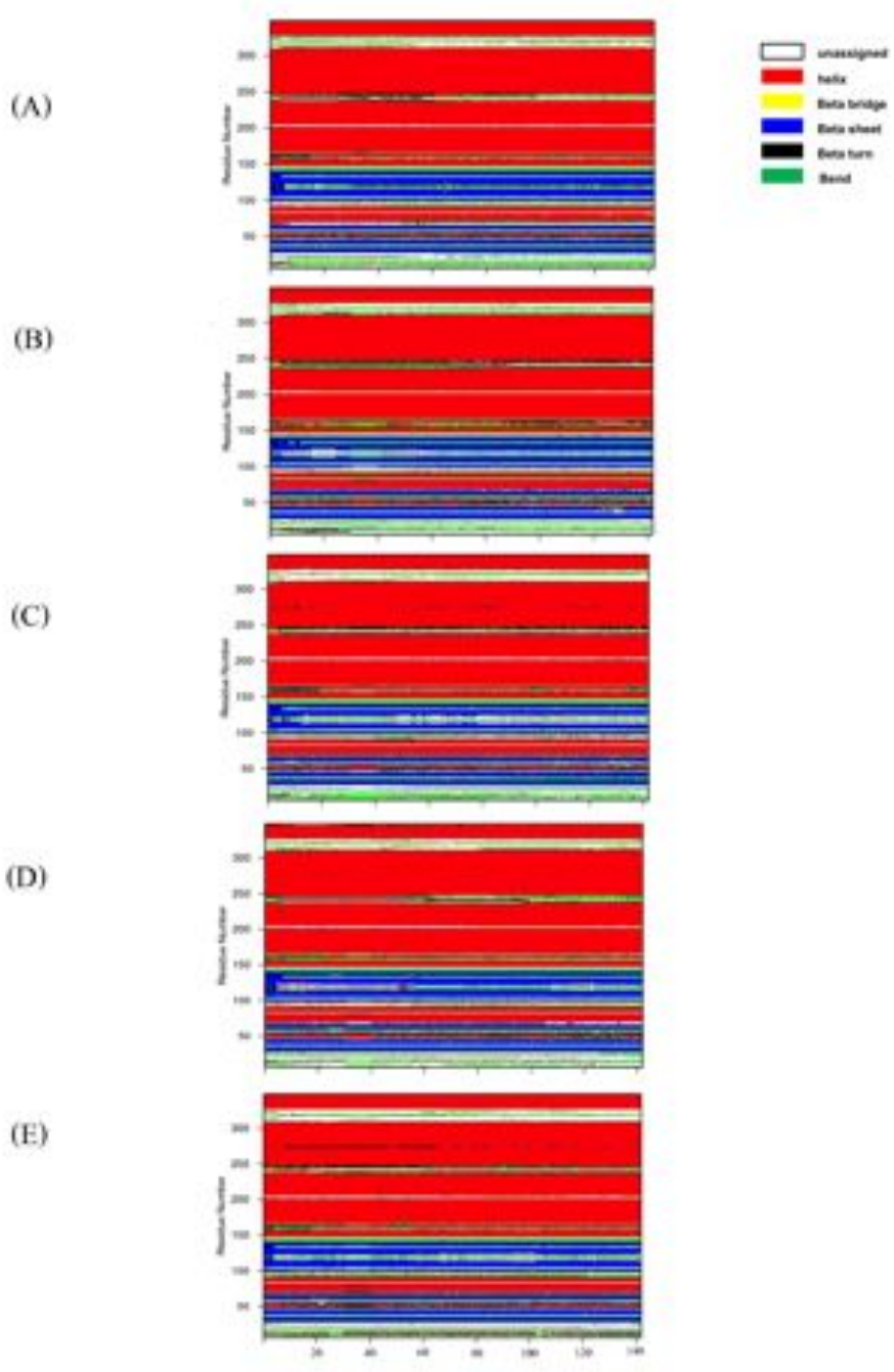

Fig 4.10 Time dependence of secondary structure of closed state (I) system for each subunit assigned by DSSP program, where alpha helix is in red, beta-sheet in blue, beta-bridge in yellow, beta-turn in black, coil in green and unassigned in white.

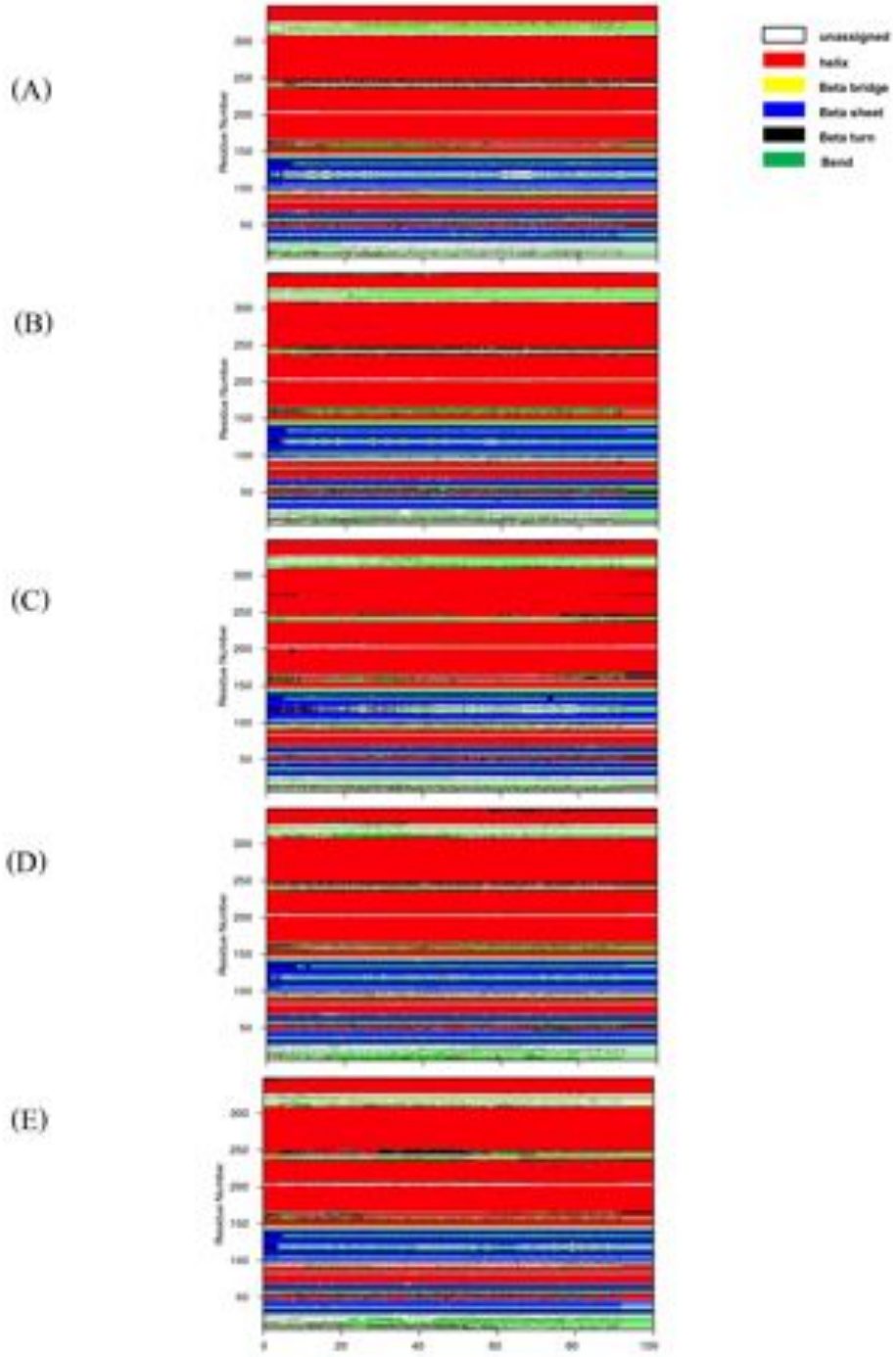

Fig 4.11 Time dependence of secondary structure of Close II for each subunit

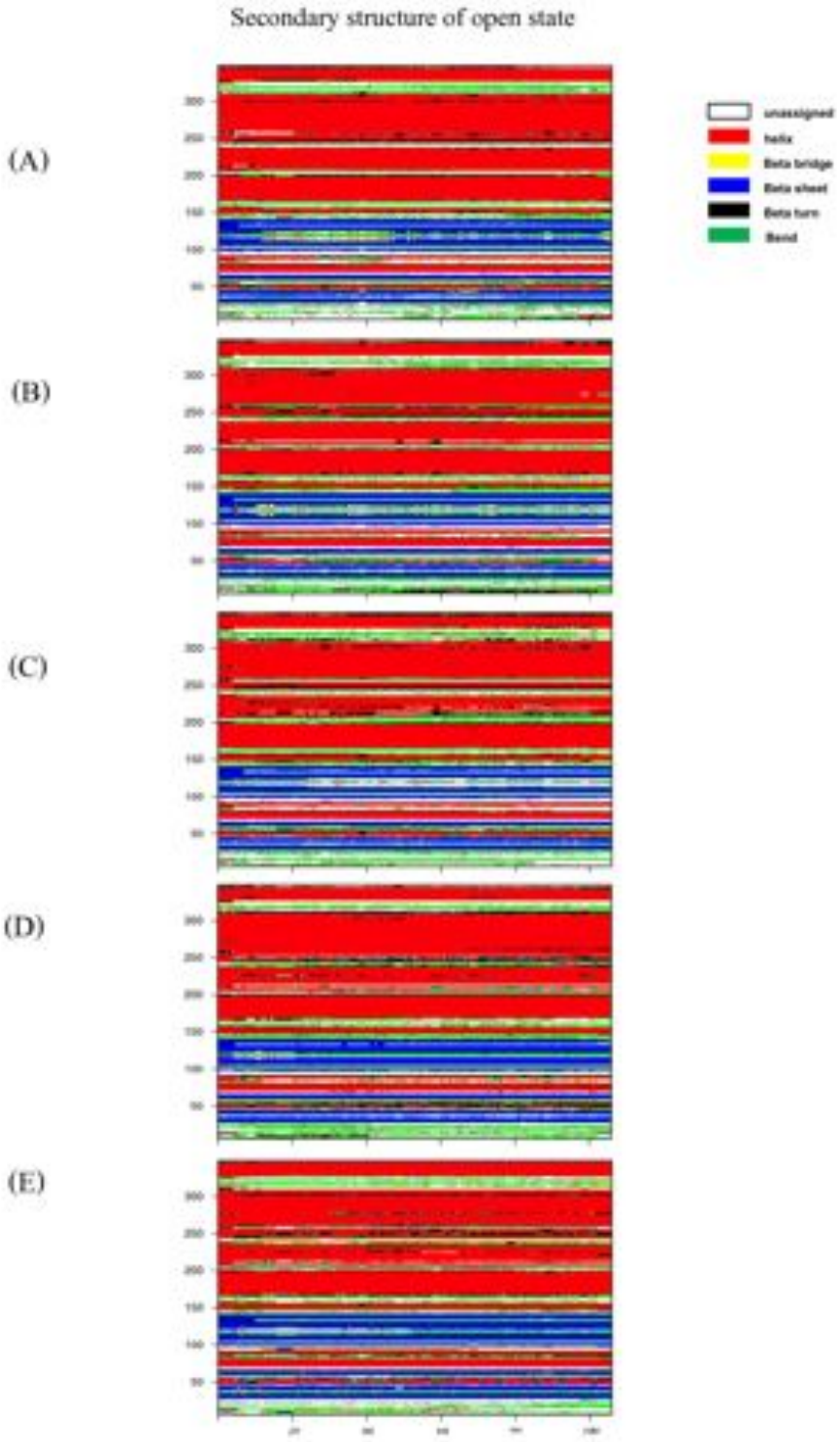

Fig 4.12 Time dependence of secondary structure of open system for each subunit

4.3 Pore radius profile by HOLE program

The pore radius of CorA along the channel interior was computed using the HOLE program. Figure 4.13 illustrates the pore radius profile average over 2ns of MD trajectory plotted as a function of membrane normal axis denoted as z-axis. The approximate transmembrane region encompasses residues from Met291 to Met313. Close I has only one binding site at the ring of Asp277 and Close II has two divalent cation binding site near Gly309 and Asp277. The average pore radius profiles of both systems are essentially identical. In Close I and Close II, ion-permeation pathway that is illustrated by the pore profile is considerably narrow and rigid in membrane bilayer. It has been found that side chains of Met291, Leu294 and Met302 of the five subunits are oriented to create hydrophobic pore constrictions with a radius of 1.5-2.0 Å. Several regions in the membrane along the permeation pathway exhibited the pore size being too narrow to allow Mg^{2+} to pass in the hydrated form.

In the open state, the permeation pathway is apparently wider. However it contains two constriction regions. The first narrow pore is located near the periplasmic loop (Met313). The second constriction is in the membrane and formed by an arrangement of Met302 and Phe306 of the five subunits. These residues might be the part of selectivity for translocation Mg^{2+} ion. The plot of the radius profile in the open state also showed a large standard deviation (error bars). This suggested that the pore interior is highly flexible compared to that of the closed conformation.

The pore hydration of Close I, Close II and Open is monitored by water distribution along the channel axis as shown in Figure 4.15. During the simulation, water entranced to the pore and dropped at Met302 and Met294 for periplasmic side and cytoplasmic side respectively. The close pore is not wide enough to allow water molecules (radius ~1.4 Å) to pass through. In contrast, the open pore was hydrated throughout the simulation. These results confirm open and closed state conformation of CorA.

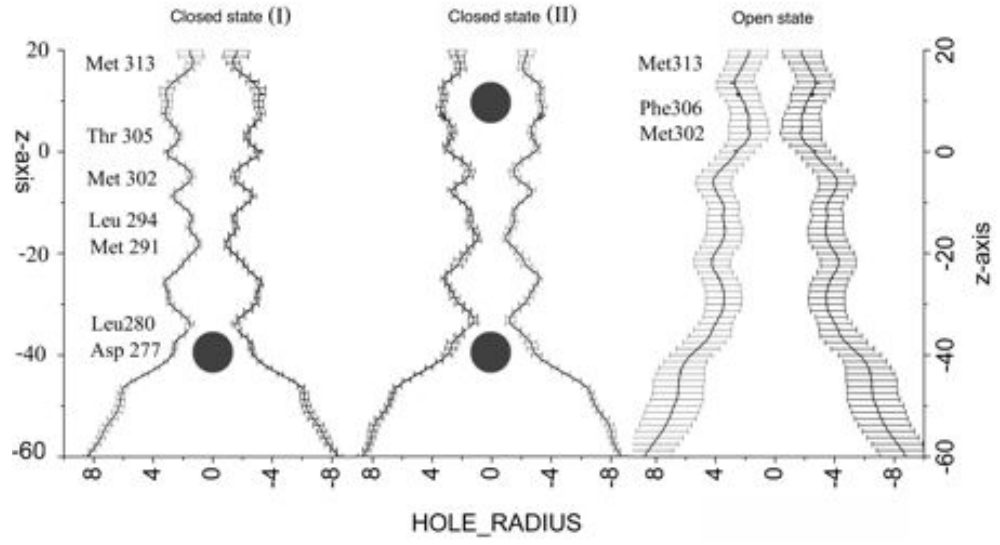

Fig 4.13 Pore diameter profiles of CorA averaged over 2ns MD trajectories of the Close I, Close II and Open simulation. The black filled circles shown in the profiles of Close I and Close II represent the starting position of Mg^{2+} of the simulation. Error bars indicate a standard deviation.

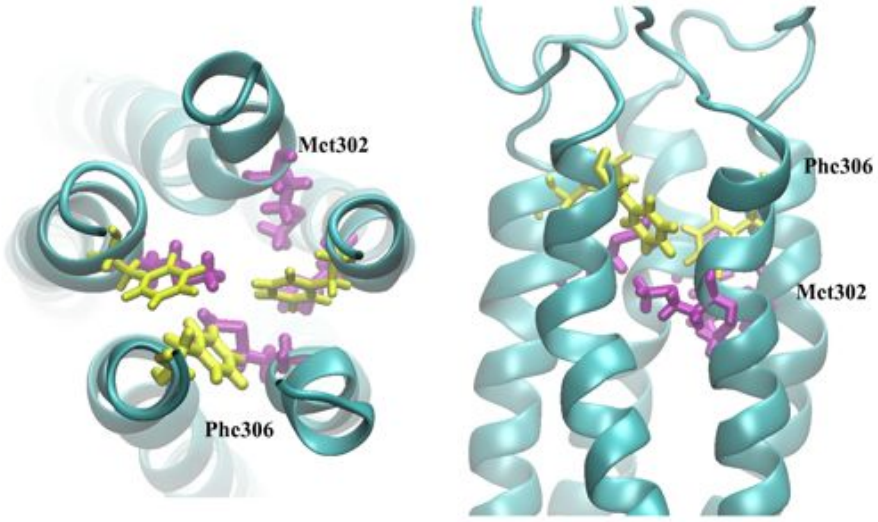

Fig 4.14 The snapshot of open pore of TmCorA at 60ns, the top and side view of TM1 helices and Met302 (purple) and Phe306 (yellow)

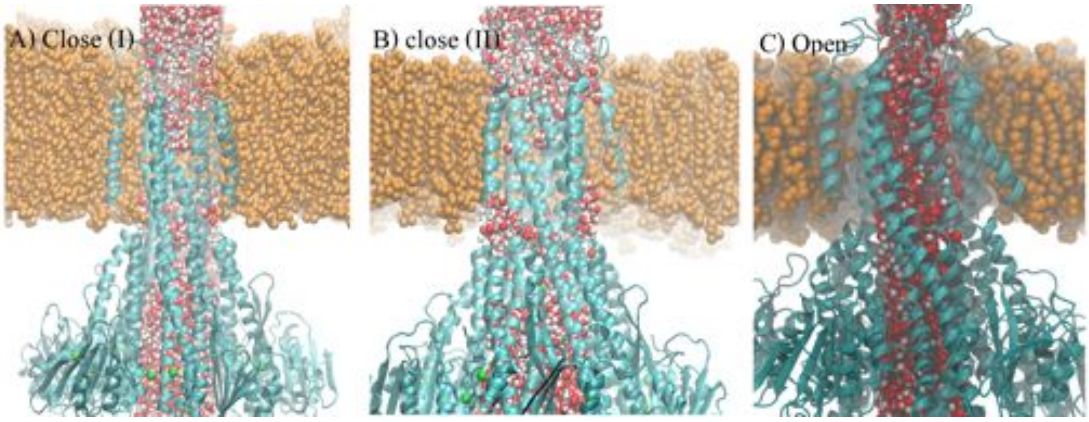

Fig 4.15 The snapshot of water in pore of TmCorA at 20ns, (A) close system (I) (B) close system (II) (C) open system

4.4 Coordination of Mg^{2+} binding site of TmCorA

All three x-ray crystal structures of TmCorA obtained in the presence of high Mg^{2+} concentration corresponded to closed state with cation binding sites[11-13]. As shown in Figure 4.16, four Mg^{2+} binding sites which have been identified from the crystal structures include two intracellular M1 and M2 sites, one near the periplasmic site (MsiteA) and one around a central permeation pathway in the cytosol (MsiteB). M1 and M2 sites located at the interface between the cytoplasmic domains have been proposed to involve in allosteric regulation of Mg^{2+} transport. Because there are two regulatory Mg^{2+} binding sites located between each monomer, a CorA pentamer has ten binding sites. It has been shown that the regulatory Mg^{2+} binding sites play an importance role as divalent cation sensor.

To provide more details about coordination of Mg^{2+} binding sites, metal-ligand coordination bonds were analyzed in terms of radial distribution function (RDF). RDF or the pair correlation function, g(r), gives the probability of finding particle at distance (r) away from reference particle. Mg^{2+} is known to favorably form a stable hexa-coordination complex with octahedral geometry. In the crystal structure, it appears that all Mg^{2+} at M1 and M2 sites were not only coordinated with amino acid but also coordinated with water molecules. Radial distribution functions (RDF) of all Mg^{2+} ions present in the protein were analyzed using MD trajectory. Close I contains 10+1 for regulatory and MsiteB magnesium. Close II has 12 Mg^{2+} binding sites including 10+1+1 for regulatory, MsiteA and MsiteB sites, respectively.

The results are shown in Table 4.1 and Table 4.2 for Close I and Close II respectively. As it can be seen, all Mg^{2+} ions have always six ligand atoms from amino acid and water. Mg^{2+} ions in M1 sites mostly coordinated with carboxyl oxygen atom of acidic residues such as Asp253 or Glu 88 or Asp 89, and also have 2-3 water molecules as ligand. His257 was found as ligand for Mg^{2+} in M1(A,B) and M1(D,E) sites. However, Mg^{2+} weakly interacts to this ligand nitrogen atom of His257 at M1(A,B) and therefore the His257 ligand was replaced by water molecules during the simulation. For Mg^{2+} coordination in M2 site, the simulation showed two ligands from the protein, Asp175 or Asp179, tightly bound to the divalent metal cation. The number of water ligands observed from the simulation is in the range from 3 to 6 molecules. It should be noted that an exchange of ligand molecules was observed for M1(B,C) and M2(B,C) sites, at which Asp253 and Asp175 of chain B were replaced by water molecules. In addition, the fully hydrated Mg^{2+} ion at M2(D,E) site was out of binding site at 34 ns of the simulation of Close II. MsiteB of close system accommodates a partial hydrated Mg^{2+} of three oxygen atoms from D277 and three and four oxygen atoms from waters for close I and close II respectively. MsiteA is found to be fully hydrated Mg^{2+} during the course of simulations.

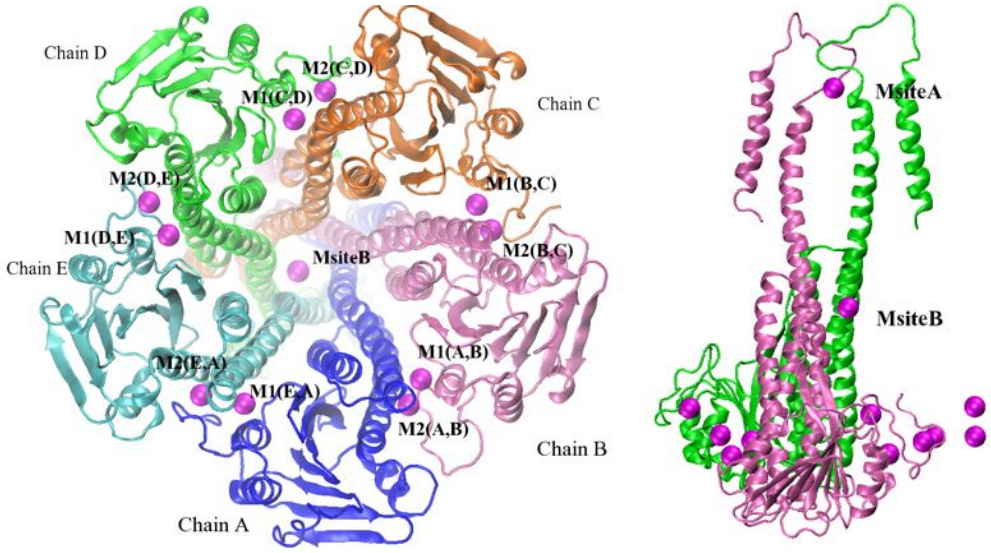

Fig 4.16 Regulatory metal binding site and permeation pore binding site of Close system (I) and (II)

The radial distribution function (RDF) of water molecules surrounding Mg^{2+} ion was computed from MD trajectory (Figure 4.17 – 4.20). RDF graph shows the highest peak located at 2 Å indicating the distance of oxygen atom away from Mg^{2+} ion in the first solvation shell. The second peak indicated the second solvation shell at 4 Å. Integration of these peaks provide the number of water molecules as shown in right axis.

Table 4.1 Magnesium coordination of Close system (I)

#Mg^{2+}	Binding site	Ligand/chain ID					
1	M1(A,B)	Asp253/A	Glu88/B	Asp89/B	Water	Water	His257/A or water
2	M2(A,B)	Asp175/A	Water	Water	Water	Water	Water
3	M1(B,C)	Asp253/B	Glu88/C	Asp89/C	Asp89/C	Water	Water
4	M2(B,C)	Asp175/B	Asp175/B	Water	Water	Water	Water
5	M1(C,D)	Asp253/C	Asp89/D	Asp89/D	Water	Water	Water
6	M2(C,D)	Water	Water	Water	Water	Water	Water
7	M1(D,E)	Asp253/D	Asp89/E	Asp89/E	Water	Water	His257/D
8	M2(D,E)	Water	Water	Water	Water	Water	Water
9	M1(E,A)	Leu85/A	Glu88/A	Asp89/A	Asp253/E	Water	Water
10	M2(E,A)	Asp175/E	Asp175/E	Asp179/E	Water	Water	Water
11	MsiteB	Asp277/D	Asp277/E	Asp277/E	Water	Water	Water

Table 4.2 Magnesium coordination of Close system (II)

#Mg^{2+}	Binding site	Ligand/chain ID					
1	M1(A,B)	Asp253/A	Glu88/B	Asp89/B	Water	Water	His257/A
2	M2(A,B)	Asp175/A	Asp179/A	Water	Water	Water	Water
3	M1(B,C)	Asp253/B	Asp253/B	Glu88/C	Asp89/C	Water	Water
4	M2(B,C)	Asp175/B	Asp175/B	Asp179/B	Water	Water	Water
5	M1(C,D)	Asp253/C	Asp253/C	Leu85/D	Asp89/D	Water	Water
6	M2(C,D)	Asp175/C	Asp179/C	Water	Water	Water	Water
7	M1(D,E)	Asp253/D	Asp253/D	Asp89/E	Asp89/E	Water	Water
8	M2(D,E)	Water	Water	Water	Water	Water	Water
9	M1(E,A)	Asp89/A	Asp89/A	Asp253/E	Asp253/E	Water	Water
10	M2(E,A)	Asp179/E	Asp179/E	Water	Water	Water	Water
11	MsiteB	Asp277/D	Asp277/E	Water	Water	Water	Water
12	MsiteA	Water	Water	Water	Water	Water	Water

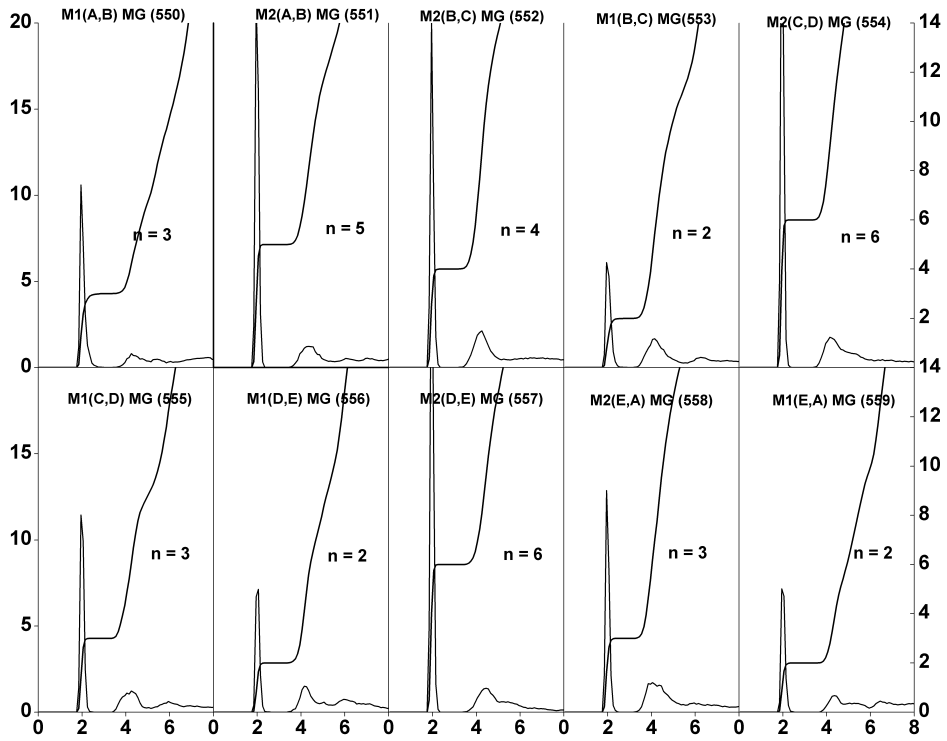

Fig 4.17 Radial distribution function of regulatory binding site of close system (I)

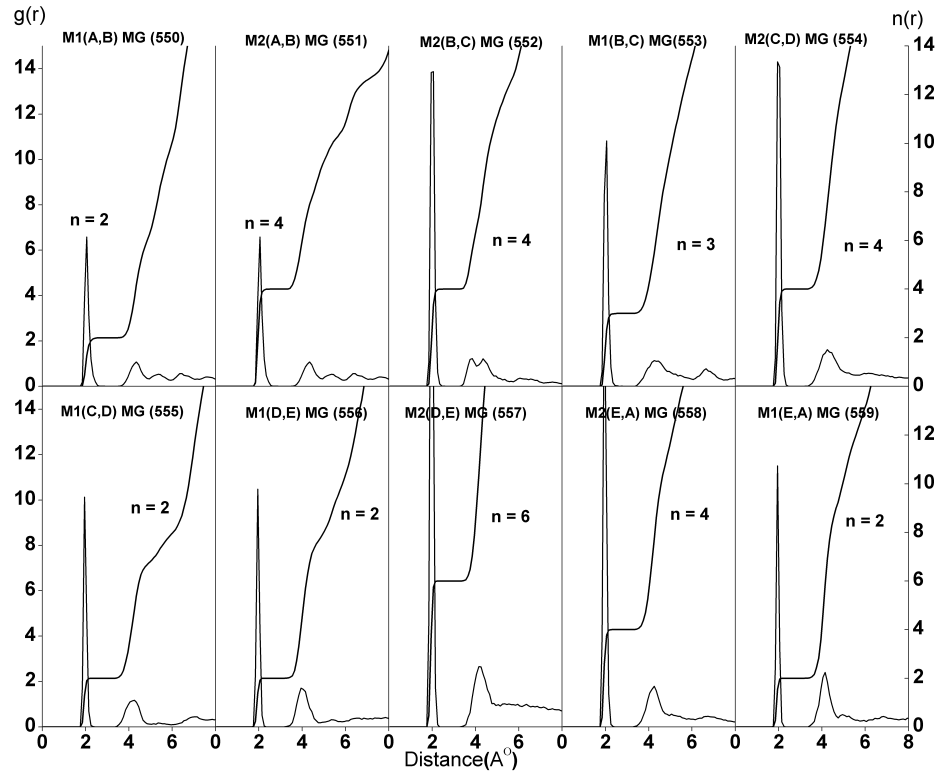

Fig 4.18 Radial distribution function of regulatory binding site of close system (II)

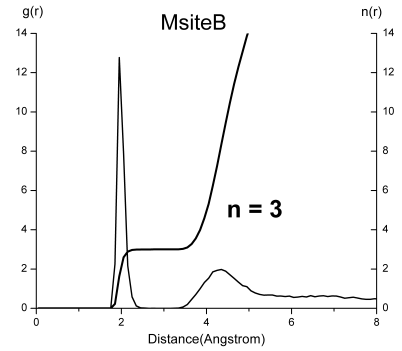

Fig 4.19 Radial distribution function of permeation binding site of close system (I)

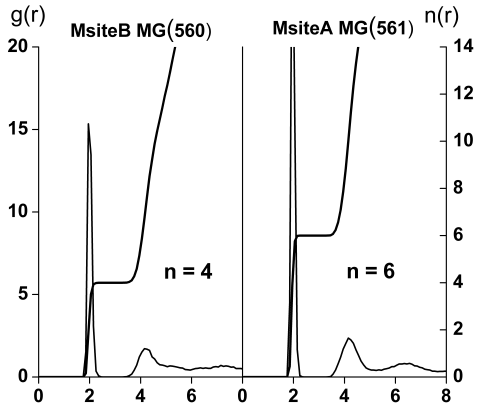

Fig 4.20 Radial distribution function of permeation binding sites in close system (II)

4.5 Steered molecular dynamics simulations

Steered molecular dynamics (SMD) simulations were performed to compute an external force required for Mg^{2+} translocation throughout the permeation pore. For preparing the simulation, Mg^{2+} ion was placed at the mouth of the pore at the starting configuration. After minimization and equilibration, six water molecules coordinated with Mg^{2+} ion. During SMD simulation, Mg^{2+} ion was being pulled by an external force toward the intracellular mouth. Because Mg^{2+} has a tight binding with water molecules, hydrated Mg^{2+} remained hexa-coordinated during the course of SMD simulation. The translocation of Mg^{2+} starts from the periplasmic pore entrance to the intracellular exit of the permeation pathway.

For constant velocity simulation, the force as a function of position in the channel was beneficial for probing troublesome region along the pathway. To

compare the barrier of permeation pathways between close and open states, the outputs of SMD force versus the z-axis position were calculated using a running average with a widow size of 500 as shown in Figure 4.21. Force peaks are correlated with specific features of ion conductive pore. The large force peaks resulting from the constraint distance for a pulling speed of 0.01 Å/ps were correlated with large barrier of the conductive pore. The force graph of closed state shows five relatively large barriers at the five hydrophobic girdles formed by Met313, Tyr311, Thr305, Met302 and Leu294, while the open force graph reveals two distinct peaks of Met313, Ile310 and Phe306. The hydrated Mg^{2+} at force peak position are represented with key residues as shown in Figure 4.22. The first largest peaks of both close and open state are associated with Met313 at the beginning of the pore. Figure 4.22 shows the positions of Met313, which protrude their hydrophobic side chains into the pore. Since Met313 is a part of the highly conserve GMN motif, it is probably the first gate of TmCorA pathway at periplasmic region. The second peak of open state SMD belonging to the Phe306 region has the same position as the Thr305 peak of closed state SMD. In open conformation, the side chain of Phe306 formed the gating inside the pore, while the side chain of Thr305 formed hydrophobic ring in closed state (Figure 4.22). After pass this narrow constriction, smoothly translocation, then, is observed because of the large pore.

Furthermore, there are minimum forces of both close and open graph near the cavity of G309 region, which is the periplasmic binding site of closed state. It has been reported that this binding site accommodated the hydrated Mg^{2+}. Payandeh et al. (2006) found that calcium ion, a week inhibitor of CorA, could enter the pore in this cavity above the hydrophobic belt formed by Thr305 and Met302. Calcium ion is not the substrate for CorA, thus they suggest that Thr305 and Met302 play a critical role of substrate selectivity. The trajectories of both SMD simulations also reveal the hydrogen bonding around the hydrated Mg^{2+} within the pore as shown in Figure 4.23.

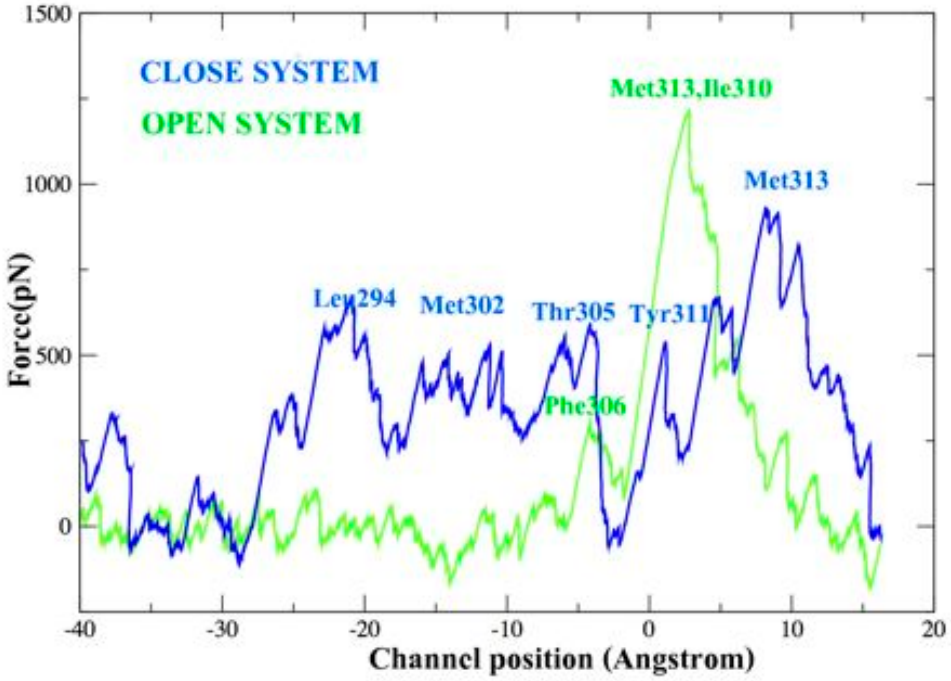

Fig 4.21 Running average of force applied on Mg^{2+} as a function of channel position (blue for the close system and green for open system)

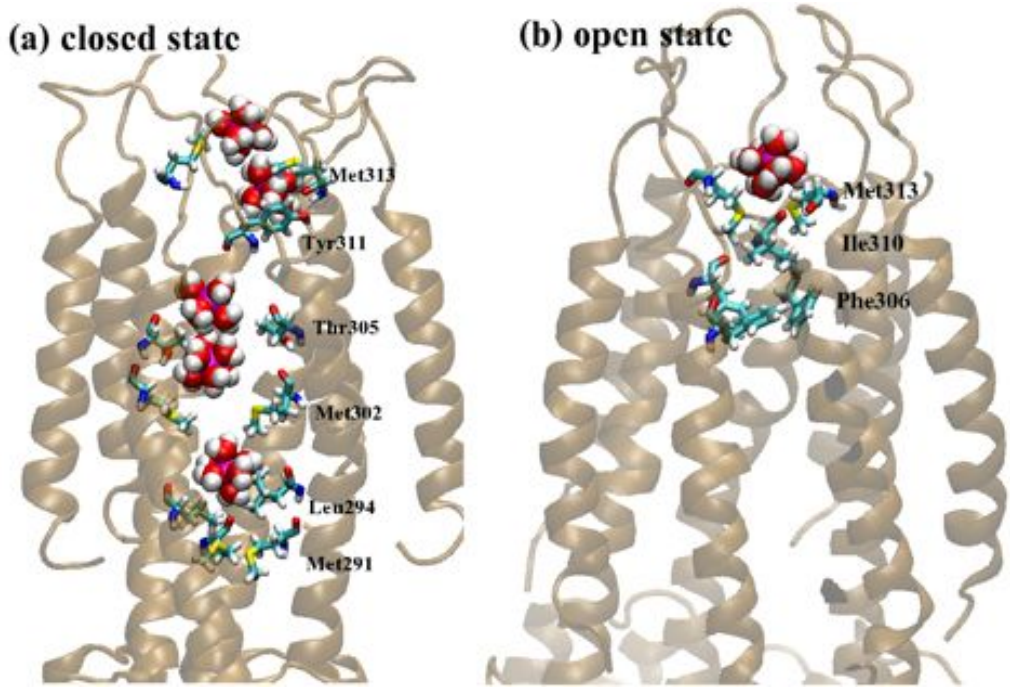

Fig 4.22 The z-trajectories of hydrated Mg^{2+} and key residues leading barrier of permeation pathway correspond to force graph as shown in Figure 4.21.

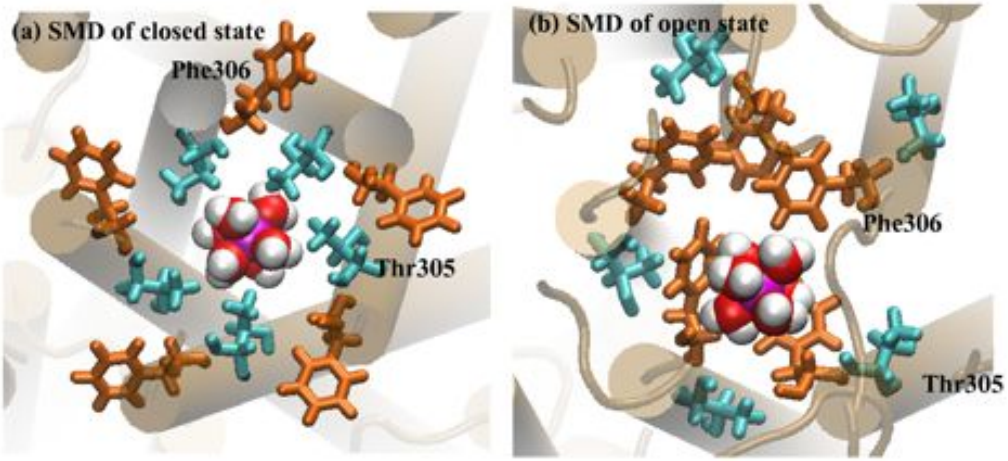

Fig 4.23 the snapshots of steered MD of closed and open state: the top view of the hydrated Mg^{2+} inside the pore which is hindered by the side chain of Thr305 (for closed-state) or Phe306 (for open-state). The hydrated Mg^{2+} are displayed in van der Waals representation; side chain of Thr305 and Phe306 are shown in licorice colored blue and orange, respectively.

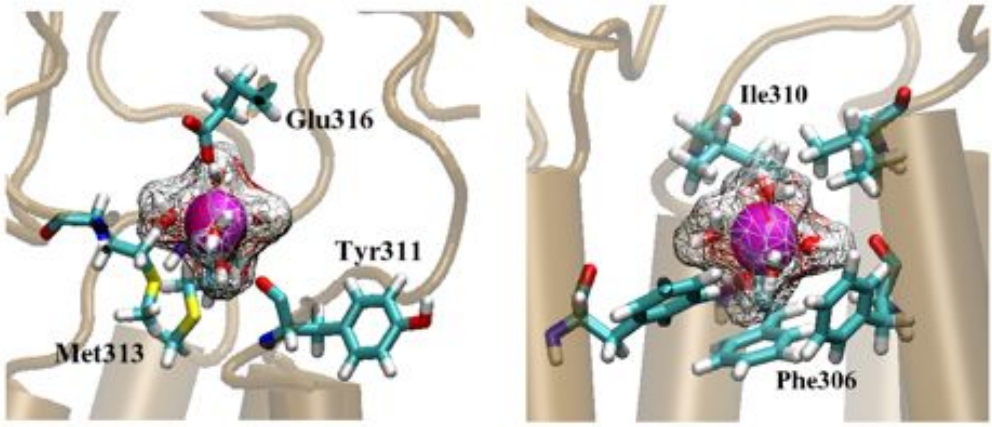

Fig 4.24 The snapshots of open SMD simulation associated two peaks of force graph. The hydrogen bond interaction between hydrated Mg^{2+} and residues of channel lining during Mg^{2+} pass through the pore

CHAPTER V
CONCLUSION

In this work, molecular dynamics simulations of CorA were performed to investigate structural and dynamics properties of its closed and open conformations. The closed-state structure is available from the crystal structure. Giving experimental EPR dataset obtained for the open-state conditions as structural restraints, a PaDSAR approach was used to drive CorA in its open conformation from the closed-state structure. The ten best structures gives RMSD of 2.12±0.54Å, suggesting a good convergence of ensemble structures. In the selected structures, stalk and TM1 helices are structurally well-defined with RMSD of 1.68±0.42Å whereas structures in the cytoplasmic domain and the periplasmic loop are disordered. Inspecting the pore size in the open conformation revealed an expansion of the inner cavity as a result of a rigid-body scissor-like motion around the kink of the stalk and TM1 helix. The diameter of the open pore is large enough for allowing the passage of hexa-hydrated Mg^{2+} in the membrane region. Nevertheless, the open model shows a narrow pore around the periplasmic loop and near Met313, Glu316 and Met318, which is likely to control Mg^{2+} translocation across the permeation pathway by the ion-selective property.

The quality of the closed and open models was assessed by means of MD simulation in hydrated phospholipid bilayer. Considering the different number and position of metal ions observed from the crystal structures in the closed state and the open model, three simulation systems were studied: the closed conformations containing 11 Mg^{2+} (Close I) and 12 Mg^{2+} (Close II) and the open conformation without Mg^{2+}. Analysis of the trajectory from 100ns MD simulation revealed different levels of structural stabilities of the closed and open conformations. It appears that the simulation of Close II showed the greatest structural stability, implying a role of metal coordination site near the conserved periplasmic GMN loop on stabilizing pentameric state of CorA. The results of the metal-free open-state simulation also revealed a tendency of CorA to lose structural symmetry of the pentamer. This finding is in good agreement with previous NMR study reporting a loss of structural symmetry of CorA

in the absence of Mg^{2+}. However, the mechanism of asymmetric structural transition is not fitted with a previously proposed gating model on a concerted motion of pore dilation. In addition, the simulation of the open conformation showed a large domain motion of the cytoplasmic domain. However, there is yet no experimental evidence to support the motion of the cytoplasmic domain.

The MD study also showed that protein dynamics in the open conformations is greater than those of the two closed-state simulations. It is anticipated that in order to facilitate CorA gating, the five subunits would arrange in a way to make less packing among the subunits in order to expand the permeation pathway. This is supported by a consistency between the RMSF data and the experimental mobility parameter obtained from SDLS/EPR technique. This result led to the conclusion that the arrangement of five monomeric subunits of CorA in its closed conformation is more compact than that of the open CorA.

An analysis of Mg-ligand coordination complex was carried out at various metal-binding sites. The results showed that in the first solvation shell all Mg^{2+} ions have always six ligand atoms belonging to either amino acid or water. It has been found that Mg^{2+} ions coordinated with more acidic residues at M1 site than those at M2 site. The simulation showed an exchange of the surrounding ligands, especially His257 and ligands at M2 sites, implying that Mg^{2+} interacts to these surrounding ligands with different binding strength.

Steered molecular dynamics was conducted to investigate an energetic barrier required to translate Mg^{2+} along the conduction pore in the closed and open-state models. The closed conformation showed several barriers for Mg^{2+} translocation from the periplasmic entrance to the cytoplamic exit of the pore. The open conformation showed high barrier forces located around the periplasic mount of the pore. This is possibly due to electrostatic interactions with glutamate residue in the loop. Once Mg^{2+} enter to the pore in the membrane region, the passage of metal ion takes place with considerably low energy. The SMD results supported the role of periplasmic loop for the ion-selective property of CorA. The present results provide more understanding of the Mg^{2+} permeation process and may guide to further study of permeation mechanism of Mg^{2+} transport in CorA.

REFERENCES

1. Romani, A. M. P. Cellular magnesium homeostasis. Archives of Biochemistry and Biophysics 512, 1(2011): 1-23.
2. Sissi, C.; Palumbo, M. Effects of magnesium and related divalent metal ions in topoisomerase structure and function. Nucleic acids research 37, 3(2009): 702-711.
3. Maguire, M.; Cowan, J., Magnesium chemistry and biochemistry. Biometals 15, 3(2002): 203-210.
4. Flatman, P. W. Mechanisms of Magnesium Transport. Annual Review of Physiology 53, 1(1991): 259-271.
5. Moncrief, M. B. C.; Maguire, M. E. Magnesium transport in prokaryotes. JBIC Journal of Biological Inorganic Chemistry 4, 5(1999): 523-527.
6. Smith, R. L.; Maguire, M. E. Microbial magnesium transport: unusual transporters searching for identity. Molecular Microbiology , 28, 2(1998): 217-226.
7. Maguire, M. E. Magnesium transporters: properties, regulation and structure. Front Biosci 11, (2006): 3149-63.
8. Dalmas, O. Magnesium selective ion channels. Biophysical journal 93, 11(2007): 3729-3730.
9. Guskov, A.; Eshaghi, S. Chapter Fourteen - The Mechanisms of Mg^{2+} and Co^{2+} Transport by the CorA Family of Divalent Cation Transporters. In Current Topics in Membranes, pp.393-414. New York : Academic Press, 2012
10. Niegowski, D.; Eshaghi, S. The CorA family: Structure and function revisited. Cellular and Molecular Life Sciences 64, 19(2007): 2564-2574.
11. Eshaghi, S.; Niegowski, D.; Kohl, A.; Molina, D. M.; Lesley, S. A.; Nordlund, P. Crystal Structure of a Divalent Metal Ion Transporter CorA at 2.9 Angstrom Resolution. Science 313, 5785(2006): 354-357.
12. Lunin, V. V.; Dobrovetsky, E.; Khutoreskaya, G.; Zhang, R.; Joachimiak, A.; Doyle, D. A.; Bochkarev, A.; Maguire, M. E.; Edwards, A. M.; Koth, C. M. Crystal structure of the CorA Mg^{2+} transporter. Nature 440, 7085(2006): 833-837.

13. Payandeh, J.; Pai, E. F. A structural basis for Mg^{2+} homeostasis and the CorA translocation cycle. EMBO J 25, 16(2006):3762-3773.
14. Maguire, M. E. The structure of CorA: a Mg^{2+}-selective channel. Current Opinion in Structural Biology 16, 4(2006): 432-438.
15. Dalmas, O.; Cuello, L. G.; Jogini, V.; Cortes, D. M.; Roux, B.; Perozo, E. Structural Dynamics of the Magnesium-Bound Conformation of CorA in a Lipid Bilayer. Structure 18, 7(2010): 868-878.
16. Moomaw, A. S.; Maguire, M. E. The Unique Nature of Mg^{2+} Channels. Physiology 23, 5(2008): 275-285.
17. Palombo, I.; Daley, D. O.; Rapp, M. The Periplasmic Loop Provides Stability to the Open State of the CorA Magnesium Channel. Journal of Biological Chemistry 287, 33(2012): 27547-27555.
18. Payandeh, J.; Li, C.; Ramjeesingh, M.; Poduch, E.; Bear, C. E.; Pai, E. F. Probing Structure-Function Relationships and Gating Mechanisms in the CorA Mg^{2+} Transport System. Journal of Biological Chemistry 283, 17(2008): 11721-11733.
19. Svidová, S.; Sponder, G.; Schweyen, R. J.; Djinović-Carugo, K. Functional analysis of the conserved hydrophobic gate region of the magnesium transporter CorA. Biochimica et Biophysica Acta (BBA) - Biomembranes 1808, 6(2011): 1587-1591.
20. Sompornpisut, P.; Roux, B.; Perozo, E. Structural Refinement of Membrane Proteins by Restrained Molecular Dynamics and Solvent Accessibility Data. Biophysical journal 95, 11(2008), 5349-5361.
21. Chakrabarti, N.; Neale, C.; Payandeh, J.; Pai, E. F.; Pomès, R. An Iris-Like Mechanism of Pore Dilation in the CorA Magnesium Transport System. Biophysical Journal 98, 5(2010): 784-792.
22. Hu, J.; Sharma, M.; Qin, H.; Gao, F. P.; Cross, T. A. Ligand Binding in the Conserved Interhelical Loop of CorA, a Magnesium Transporter from Mycobacterium tuberculosis. Journal of Biological Chemistry 284, 23(2009): 15619-15628.

23. Kucharski, L. M.; Lubbe, W. J.; Maguire, M. E. Cation Hexaammines Are Selective and Potent Inhibitors of the CorA Magnesium Transport System. Journal of Biological Chemistry 275, 22(2000): 16767-16773.

24. Moomaw, A. S.; Maguire, M. E. Cation Selectivity by the CorA Mg^{2+} Channel Requires a Fully Hydrated Cation. Biochemistry 49, 29(2010): 5998-6008.

25. Mulholland, A. J., Introduction. Biomolecular simulation. Journal of The Royal Society Interface 5, (2008): 169-172.

26. Dodson, G. G.; Lane, D. P.; Verma, C. S. Molecular simulations of protein dynamics: new windows on mechanisms in biology. EMBO reports 9, 2(2008): 144-150.

27. van der Kamp, M. W.; Shaw, K. E.; Woods, C. J.; Mulholland, A. J. Biomolecular simulation and modelling: status, progress and prospects. Journal of The Royal Society Interface 5, (2008): 173-190.

28. Dror, R. O.; Dirks, R. M.; Grossman, J. P.; Xu, H.; Shaw, D. E. Biomolecular Simulation: A Computational Microscope for Molecular Biology. Annual Review of Biophysics 41, 1(2012): 429-452.

29. Allen, M. P. Introduction to molecular dynamics simulation.

30. González, M. A. Force fields and molecular dynamics simulations. JDN 12, (2011): 169-200.

31. Monticelli, L.; Tieleman, D. P. Force Fields for Classical Molecular Dynamics. In Biomolecular Simulations, pp.197-213. : Humana Press, 2013.

32. Cisneros, G. A.; Babin, V.; Sagui, C. Electrostatics Interactions in Classical Simulations #. In T Biomolecular Simulations, pp.243-270 ,2012.

33. Hug, S., Classical Molecular Dynamics in a Nutshell. In Monticelli, L.; Salonen, E., Eds. Biomolecular Simulations, pp.127-152. : Humana Press, 2013.

34. Quigley, D.; Probert, M. I. J., Langevin dynamics in constant pressure extended systems. The Journal of Chemical Physics 120, 24(2004): 11432-11441.

35. Phillips, J. C.; Braun, R.; Wang, W.; Gumbart, J.; Tajkhorshid, E.; Villa, E.; Chipot, C.; Skeel, R. D.; Kalé, L.; Schulten, K., Scalable molecular dynamics with NAMD. Journal of Computational Chemistry 26, 16(2005): 1781-1802.

36. Darden, T.; York, D.; Pedersen, L., Particle mesh Ewald: An N [center-dot] log(N) method for Ewald sums in large systems. The Journal of Chemical Physics 98, 12(1993): 10089-10092.

37. Humphrey, W.; Dalke, A.; Schulten, K., VMD: Visual molecular dynamics. Journal of Molecular Graphics 14, 1(1996): 33-38.

38. Hsin, J.; Arkhipov, A.; Yin, Y.; Stone, J. E.; Schulten, K., Using VMD: An Introductory Tutorial. In *Current Protocols in Bioinformatics*, John Wiley & Sons, Inc.: 2002.

39. Kalé, L.; Skeel, R.; Bhandarkar, M.; Brunner, R.; Gursoy, A.; Krawetz, N.; Phillips, J.; Shinozaki, A.; Varadarajan, K.; Schulten, K., NAMD2: Greater Scalability for Parallel Molecular Dynamics. Journal of Computational Physics 151, 1(1999): 283-312.

40. MacKerell, A. D.; Brooks, C. L.; Nilsson, L.; Roux, B.; Won, Y.; Karplus, M., {CHARMM}: The Energy Function and Its Parameterization with an Overview of the Program. In Schleyer, Ed. John Wiley & Sons: Chichester: 1998; Vol. 1, pp 271-277.

41. Smart, O. S.; Neduvelil, J. G.; Wang, X.; Wallace, B. A.; Sansom, M. S. P., HOLE: A program for the analysis of the pore dimensions of ion channel structural models. Journal of Molecular Graphics 14, 6(1996): 354-360.

42. Andersen, C. A.; Bohr, H.; Brunak, S., Protein secondary structure: category assignment and predictability. FEBS Letter*s* 507, 1(2001): 6-10.

43. Sompornpisut, P.; Roux, B.; Perozo, E., Structural refinement of membrane proteins by restrained molecular dynamics and solvent accessibility data. Biophys J 95, 11(2008): 5349-61.

APPENDICES

Appendix A.

NAMD input file

```
#############################################################
## JOB DESCRIPTION                                         ##
#############################################################

# MD simulation of membrane protein at 300K
# embedded in POPC membrane, ions and water.
# Protein released. PME, Constant Pressure/Area.

#############################################################
## ADJUSTABLE PARAMETERS                                   ##
#############################################################

margin 2.5;
structure          ../02membrane/ionized.psf
coordinates        ../02membrane/ionized.pdb
outputName         md-30

set temperature    300

# Continuing a job from the restart files
if [11] {
set inputname      md-29
binCoordinates     $inputname.restart.coor
binVelocities      $inputname.restart.vel  ;# remove the "temperature" entry if you use
this!
extendedSystem            $inputname.restart.xsc
}

firsttimestep     29000000


#############################################################
## SIMULATION PARAMETERS                                   ##
#############################################################

# Input
paraTypeCharmm          on
parameters          ../par_all27_prot_lipid.inp

# NOTE: Do not set the initial velocity temperature if you
# have also specified a .vel restart file!
# temperature         $temperature
```

```
# Periodic Boundary Conditions
# NOTE: Do not set the periodic cell basis if you have also
# specified an .xsc restart file!
if {1} {
cellBasisVector1    137.    0.   0.
cellBasisVector2     0.   137.   0.
cellBasisVector3     0.    0.  156.
cellOrigin        -0.06553388386964798 -0.0815470740199089 -25.110055923461914
}
wrapWater           on
wrapAll             on


# Force-Field Parameters
exclude             scaled1-4
1-4scaling          1.0
cutoff              12.
switching           on
switchdist          10.
pairlistdist        13.5


# Integrator Parameters
timestep            2.0  ;# 2fs/step
rigidBonds          all  ;# needed for 2fs steps
nonbondedFreq       1
fullElectFrequency  2
stepspercycle       20


#PME (for full-system periodic electrostatics)
if {1} {
PME                 yes
PMEGridSizeX        140
PMEGridSizeY        140
PMEGridSizeZ        156
}


# Constant Temperature Control
langevin            on    ;# do langevin dynamics
langevinDamping     1     ;# damping coefficient (gamma) of 5/ps
langevinTemp        $temperature

# Constant Pressure Control (variable volume)
if {1} {
useGroupPressure      yes ;# needed for 2fs steps
useFlexibleCell       yes  ;# no for water box, yes for membrane
useConstantArea       yes  ;# no for water box, yes for membrane
```

```
langevinPiston       on
langevinPistonTarget  1.01325 ;#  in bar -> 1 atm
langevinPistonPeriod  200.
langevinPistonDecay   50.
langevinPistonTemp    $temperature
}


restartfreq       1000     ;# 1000steps = every 2ps
dcdfreq           1000
xstFreq           1000
outputEnergies      500
outputPressure      500


# Fixed Atoms Constraint (set PDB beta-column to 1)
#if {0} {
#fixedAtoms         on
#fixedAtomsFile      nottails.fix.pdb
#fixedAtomsCol       B
#fixedAtomsForces    on
#}

#############################################################
## EXTRA PARAMETERS                                        ##
#############################################################

# Put here any custom parameters that are specific to
# this job (e.g., SMD, TclForces, etc...)

#############################################################
## EXTRA PARAMETERS                                        ##
#############################################################

# Put here any custom parameters that are specific to
# this job (e.g., SMD, TclForces, etc...)

#constraints on
#consexp 2
#consref ../02membrane/ionized.pdb
#conskfile protein-popcwi.fixprot
#conskcol B
#margin 3

#tclforces on
#set waterCheckFreq            100
#set lipidCheckFreq            100
#set allatompdb               ../02membrane/ionized.pdb
#tclForcesScript              keep_water_out.tcl
```

```
#eFieldOn yes
#eField 0 0 -0.155


#####################################################################
## EXECUTION SCRIPT                                 ##
#####################################################################

# Minimization
#if {0} {
#minimize           2000
#reinitvels         $temperature
#}

run 1000000 ;# 2.0 ns
```

Appendix B.

HOLE input file

```
! HOLE PROGRAM
! input file for CorA  pentamer structure
! note everything preceeded by a "!" is a comment and will be ignored by HOLE
!
! follow instructions in 000_README to run this job
!
! first cards which must be quoted
! (note that HOLE is case insensitive (except file names)
coord  tmp_prot.pdb        ! Co-ordinates in pdb format
radius /fs/home/bio017/hole/hole2/rad/simple.rad     ! Use simple AMBER vdw radii
cvect 0 0 1    !   vector which lies in the direction of the channel/pore
cpoint 0.0 0.0 0.0
!
! now optional cards
sphpdb hole.sph            ! pdb format output of hole sphere centre info
                                ! (for use in sph_process program)
pltout hole.qpt             !
endrad 20.                      ! This is the pore radius that is taken
                        ! as an end
molqpt stick.qpt              ! qpt file of the molecule
                        ! (stick plot in one colour)
```

VITAE

Personal Data:

First Name: Ms. Pattama **Last Name:** Wapeesittipan

Date of birth: April 24, 1988 **Height:** 155 cm.

Weight: 43 kg. **Citizenship:** Thai

Religion: Buddhism **Domicile/Habitation:** Nakhornpathom

Gender: Female **Primary Phone:** (+66) 08-5979 6328

E-mail address: pat_kadae@hotmail.com

Home Address: 44/13 M.2 T. Nongdindeang A.Muang

State/Province: Nakornpathom **Postal Code:** 73000

Country: Thailand

Education:

2010-Present: Master's Degree in Science, Major Chemistry (Physical chemistry) Chulalongkorn University, Thailand, GPA. 3.62/4

2006-2009: Bachelor's Degree in Science, Major Chemistry, Mahidol University, Thailand, GPA. 3.53/4

2003-2005: High School from Mahidolwittayanusorn, Nakhornpathom, Thailand GPA. 3.67/4.00

Scholarship:

2006-Present: Development and Promotion of Science and Technology Talents Project (DPST)

Research Interest:

2010-Present: Structural and dynamical properties of voltage sensor domain of activated and resting potassium channel in lipid bilayer by molecular dynamics simulation

2009: Investigation of Annexin A5 Structure That Binds with Phosphatidylserine in Lipid Bilayer using Molecular Dynamic Method